NASA Technical Memorandum 4336

Flight Vehicle Thermal Testing With Infrared Lamps

Roger A. Fields

JANUARY 1992

NASA

NASA Technical Memorandum 4336

Flight Vehicle Thermal Testing With Infrared Lamps

Roger A. Fields
Dryden Flight Research Facility
Edwards, California

National Aeronautics and
Space Administration

Office of Management

Scientific and Technical
Information Program

1992

FLIGHT VEHICLE THERMAL TESTING WITH INFRARED LAMPS

Roger A. Fields

NASA Dryden Flight Research Facility
Edwards, California

ABSTRACT

The verification and certification of new structural–material concepts for advanced high-speed flight vehicles relies greatly on thermal testing with infrared quartz lamps. The basic quartz heater system characteristics and design considerations are presented. Specific applications are illustrated with tests that were conducted for the X-15, the Space Shuttle, and YF-12 flight programs.

INTRODUCTION

The use of infrared (IR) quartz heaters is an accepted and widely used method of realistically simulating the effects of aerodynamic heating on advanced high-speed flight vehicle structural test components. Thermal ground testing of components or entire flight vehicles can also use other means of heating such as graphite heaters [1], arc jets, lasers, high-temperature tunnels, and low-speed convective heating (i.e., Concorde tests in England, [2]). However, IR lamps offer the most efficient (approximately 90 percent) and widely diverse method of testing to validate structural–material concepts and verify analytical codes.

Infrared energy produces electromagnetic radiation just below the visible spectrum, mostly at wave lengths from 0.5 to 2 μ. The radiation can easily be focused on small areas for maximum heat flux and temperatures, or it can be distributed over the surfaces of large test articles to duplicate flight heating variations.

There is a significant difference between aerodynamic and IR heating [3,4]. In-flight aerodynamic heating is a function of the difference between the recovery temperature and the component surface temperature. Laboratory radiant heating is a function of the difference between the quartz heater temperature to the fourth power and the surface temperature to the fourth power. An appreciation for this fundamental difference is necessary in the design of IR heater systems. For instance, proper distribution of quartz lamps in a system may be required to accommodate this difference, particularly in locations where there is a significant heat sink.

This paper describes the components of a basic quartz lamp heating system and discusses design considerations. In addition, the design factors that affect the heating system power requirements are presented together with a simplified method for calculating power requirements. The applications of IR quartz lamp heating to the X-15, Space Shuttle, and YF-12 flight programs are also discussed.

INFRARED HEATER BASICS

Quartz Lamps

The quartz lamps commonly used for IR heating tests consist of a tungsten filament enclosed in a quartz glass tube. These tubes are approximately 3/8 in. in diameter and of varying lengths (Fig. 1). The rated wattage of the lamps can be user selected to meet the specific test requirements. Figure 2 shows the characteristics of a 200 W/in. T-3 10-in. lighted length quartz lamp with high-temperature end seals [3,4]. As shown, this lamp produces 2000 W at rated voltage and 6000 W at double rated voltage. The lamps offer the most efficient heating when operated at the highest possible temperature. Operating at rated voltage, usually 240 V, the lamp filaments reach nearly 4000 °F. If the lamps are operated at double rated voltage or 480 V, the filaments can reach 5400 °F. The higher voltage and temperatures, however, can shorten the lamp life. For instance, temperatures in excess of 1000 °F on high-temperature end seals or quartz envelope temperatures above 1800 °F can produce premature lamp failure. In addition, the very high temperatures can cause the lamp filaments to evaporate and redeposit on the quartz envelope, reducing optical clarity, increasing the quartz temperature, and decreasing the lamp efficiency. Quartz lamps typically are quite durable and their life, for most cases, can be a few hours to several hundred hours.

Reflector Types

The types of reflectors used in a test setup vary depending upon the severity of the heating requirements. In general, there are three classes of reflectors employed to direct the radiant energy from the lamps to the test article. For low-temperature tests (usually less than 800 °F), a simple polished metal reflector (Fig. 3) will work satisfactorily. The

reflectors shown were assembled to heat the forebody section of a YF-12 aircraft [5]. These heaters were made of type 310 stainless-steel sheets that were 0.075-in. thick. The sheets were bent to conform to the contour of the airplane. Because a reflector of this type gets hot, it is necessary to leave gaps between each panel to allow for thermal expansion. Figure 4 shows a typical panel attachment scheme which provides for panel adjustment in all directions and still allows unrestrained thermal expansion. Figure 5 is a closer view of the back side of a reflector. The small metal clips used to support the quartz lamps can be seen as well as a few of the swivel attachment rods. For slightly higher temperatures (1500 °F), gold plated stainless-steel reflectors (Fig. 6) can be used. These reflectors [4], as with the previous ones, are passively cooled with back side radiation and natural convection. These units have air cooling for the ends of the quartz lamps. For higher temperatures (above 1500 °F), it is necessary to use either active cooling or a heat resistant material such as ceramic (foamed silica). In Fig. 7, an edge view of a water cooled reflector is shown. The reflector is made from polished aluminum with water distributed through manifolds to passages in the back side. Although this reflector was not designed with any cooling for the lamp and seals, a copper line was added to provide that function. Figure 8 shows a large array of the water cooled reflectors used to heat a test article to 1900 °F.

Figure 9 shows a specially designed, curved water cooled reflector which was used to heat a portion of a component to 2000 °F. The unit also provided for lamp end cooling by way of conduction.

Many test setups use ceramic reflectors (Fig. 10) which operate at very high temperatures without the need for cooling. The reflectivity of these units is much less than the previously discussed reflectors, so the initial efficiency at low temperatures is less. At higher temperatures, the surface absorbs sufficient energy so that it begins to reradiate and improve the efficiency. The reradiation is a longer wavelength which is absorbed by the quartz tubes, and hence creates a problem of lamp heating. Figure 11 shows a test setup with ceramic reflectors operating at 2500 °F.

In addition to directing the radiation, the reflectors may be required to cool the quartz lamp tubes and end seals. Such a unit is shown in Fig. 12. The reflector body is water cooled polished aluminum and the quartz lamps radiate through quartz windows which form a chamber for circulating air for cooling the lamp tubes and end seals. The windows also prevent the lamp cooling gas from impinging on the test article and disturbing the applied heat distribution. This heater can produce radiant energy up to 100 KW/ft^2 on a test article surface. Figure 13 shows lamps damaged by heat as a result of insufficient cooling air.

Power Requirements

The radiant energy or heat flux provided to a test specimen is dependent upon the entire test system, which is unique for each test setup. In addition to the quartz lamps, the test system includes (1) the type and efficiency of the reflector used to direct or focus the lamp radiation, (2) lamp-to-lamp spacing, (3) lamp-to-specimen distance, (4) boundary conditions (end effects), (5) test specimen surface emissivity, (6) convection (natural or forced) around the test article, (7) test specimen–setup discontinuities, such as heat sinks or variable geometry, and (8) possibly a moveable test article. These factors determine the electrical power requirements of a system, the maximum temperatures, and the maximum heating rates which can be achieved on any given test component. Typically, temperatures of 2000 °F to 3000 °F, rates of 100 °F/sec to 150 °F/sec, and heat fluxes up to (80 Btu/(ft^2-sec)) are easily achievable.

The equation [3] for calculating the available heat flux for an IR radiation heater can be written as

$$\dot{q}_A = \dot{q}_{\max}(\dot{q}_{T_0}/\dot{q}_{T_n}) - \dot{q}_{\text{loss}} - \dot{q}_{\text{end eff}}$$

where

$\dot{q}_{\max}$ = maximum power output of the quartz lamps in Btu/ft^2-sec

$\dot{q}_{T_0}/\dot{q}_{T_n}$ = ratio of radiant heat flux from the lamp filament at a specimen temperature of T_0 to the heat flux received by a specimen at a temperature of T_n

$\dot{q}_{\text{loss}}$ = heat flux loss of heater system in Btu/ft^2-sec

$\dot{q}_{\text{end eff}}$ = end-effects heat flux loss caused by heater design in Btu/ft^2-sec

The ratio of radiant heat flux ($\dot{q}_{T_0}/\dot{q}_{T_n}$) is derived from the difference between the test specimen surface temperature and the quartz lamp filament temperature. This ratio is shown in Fig. 14. The heat flux loss of the heater system ($\dot{q}_{\text{loss}}$) includes the losses caused by radiation, conduction, and convection. Usually, each of these losses must be calculated separately. These calculations are not free from errors, since it is necessary to make several assumptions to perform the calculations. To circumvent the time consuming process of calculation of heat losses resulting from each mode of heat transfer, an empirical curve of the total heat flux loss as a function of specimen temperature was derived from past heating tests using water cooled polished aluminum reflectors and stainless-steel reflectors. This curve is shown in Fig. 15 and is based on a specimen emissivity of approximately 0.85. Since the heating tests used to derive this curve were conducted to only 2500 °F, the curve is verified up to that temperature only, and the part of the curve from 2500 °F to 4000 °F is an extrapolation. As previously indicated, this curve represents the heating loss from radiation, conduction, and convection, but does not consider heat loss caused by end effects.

End effects on the boundaries of IR heater systems can be a major source of temperature error. The problem and

some potential solutions are shown in Fig. 16. The data for this figure were calculated using a lamp flux computer program [6]. Figure 16 shows the calculated heat flux received by the first 10 in. of the test specimen for various reflector lamp arrangements. Curve 1 shows the heat flux when the reflector ends at X = 0, and there are no added lamps and no end reflector. Curves 2, 3, and 4 were the same as curve 1, with the following exceptions

- Curve 2 - The reflector and lamps were extended 10 in. beyond the specimen surface,
- Curve 3 - an end reflector was added, and
- Curve 4 - lamps were added near X = 0.

Curve 5 is the same as curve 3 except that additional lamps were installed. This figure is not intended to present all the possible heater designs to eliminate or to minimize end effects. The results shown illustrate that boundary conditions are a serious problem that must be considered when designing IR radiation heaters. Based on the results shown in this figure, it can be concluded that as a minimum, the reflector must extend approximately 10 in. beyond the test specimen. In addition, an end reflector is required if the heat loss resulting from end effects is to be kept to a reasonable amount.

Figure 17 shows the power required as a function of heater area for specimen temperatures up to 3800 °F and heating rates from steady state (SS) up to 10 Btu/ft^2-sec. The calculations were made for a specimen emissivity of 0.85. At very high temperatures (3500 °F to 3800 °F), the slope of the curve is such that the heater area is quite small.

The quartz lamps are generally grouped or electrically wired together into zones [3]. Each zone is controlled to provide a specified temperature–heat-flux time history. Control methods vary from manual control to sophisticated computer controlled closed-loop systems with complex algorithms [7,8]. The latter method is mandatory for tests with a large number of control zones.

The data acquisition and control system currently in use at the NASA Dryden Thermostructures Research Facility [8,9] is summarized in Fig. 18. The unique feature of this system is its ability to conduct real-time simulations of thermal load on aerospace vehicle structures. With quartz lamps placed around the test specimen, the surface temperature within each zone of lamps is forced to follow a desired time history, based on feedback from a control thermocouple. An adaptive algorithm is used to compute commands to silicon controlled rectifier power controllers. As many as 512 independent thermal zones can be controlled to distribute up to 20 MW of available power. The real-time system resources may be dedicated to a single test or may be shared among as many as three autonomous test activities conducted simultaneously.

Surface Emissivity

The effects of surface emissivity on the power required for a radiation heating system is illustrated in Fig. 19. Part of the total radiant heat flux from the heater is absorbed by the test specimen and the remainder of the heat flux is reflected. Since absorptivity is equal to emissivity, the amount of the heat absorbed depends on the emissivity of the test specimen and the heat reflected depends on the reflectivity of the test specimen. Since emissivity plus reflectivity equals 1.0, it follows that the minimum power required will occur when the emissivity of the test specimen is equal to 1.0. Likewise, the maximum power will be required when the reflectivity is 1.0. The emissivity of the test specimen must be uniform if consistent results are to be obtained from IR heating tests.

Combined Heating and Loading

A common problem when dealing with hot structures testing is how to apply mechanical loads to a structure simultaneously with applied IR heating. Examples of some approaches include (1) hard points may be designed into a test structure for load introduction [10,11], (2) external load pads can be used to distribute load into the structure [4], (3) whipple-trees can be used to distribute load to the test article through discrete attachment points [12], and (4) buffer bays or load extensions may be included with the test article design to provide load through an adjoining structure. No matter which approach is selected, interference with the IR heater system and the desired temperature distribution will be encountered. Consequently, early planning during the design of structural test components for combined loading and heating will result in big dividends.

APPLICATIONS

X-15 Wing

The X-15 wing (Fig. 20) was a short-span, thin, low-aspect ratio, multispar structure. It had three main ribs: a root rib, a midspan rib, and a tip rib. The leading edge was a segmented slug or heat sink having a constant radius. The wing-to-fuselage attachments consisted of five A-frame assemblies which were an integral part of the wing. The wing skins, tip rib, front spar, and structure forward of the front spar were constructed of Inconel-X®; the remainder of the wing structure was titanium alloy. The wing is shown in the condition it was received, after removal from the aircraft. The nonuniformity of the wing-surface emissivity is obvious. A portion of the upper surface quartz heater system is shown in a raised or open position.

Preliminary heating tests [13] showed discrepancies between the simulation temperatures measured within each zone, other than control thermocouples, and with calculated temperatures. The lack of uniformity in the surface emissivity was the most likely problem. The wing is shown in Fig. 21 with a fresh coat of high-emissivity paint, which solved the anomalies.

The quartz lamps in the IR heater system for the wing were divided into 24 upper and lower surface zones, as

® Inconel is a registered trademark of International Nickel Company, Huntington, West Virginia.

shown in Fig. 22. Two additional zones were added to provide the necessary heat flux to the leading-edge area. There were more zones chordwise than spanwise to better simulate the in-flight surface temperature gradients. Figure 23 shows a cross-section of the wing and IR heater at a root station. Since the wing structure does not represent a uniform heat sink, the additional heat flux to match that imposed in flight and which is required by the highest mass locations (leading edges and primary spars) was provided by concentrating lamps over those areas. Dividers between zones were required in some locations because of the wide variation in chordwise heat flux. Without the dividers, a thermal control problem known as cross-talk [6] may exist. In that case, interference heating from a higher temperature zone can prevent a lower temperature zone from being controlled properly.

There is a major problem that occurs when applying mechanical loads during a heating simulation. Making an attachment to a structure without adding a heat sink which creates thermal stresses that are unwanted or damaging, or both. It is also necessary to design the loading mechanism to cause minimum interference to the heating system. A substantial load was applied directly to the wing test structure [12] through a 0.75-in. wide, 0.040-in. thick, 4130 steel corrugated strip at the midspan rib location (Fig. 24). This attachment caused a minimum heat sink in contact with the surface of the test structure. Rivets were removed from the wing, and the corrugated strip was fastened with blind rivets through the resulting holes. Cables were attached to the tops of the corrugations and passed through the reflector with a minimum of alteration to the heating system. The cables were thermally insulated to prevent them from becoming overheated as they passed between the heat lamps. No detrimental effects were observed in the flight heating profile on any part of the structure resulting from the loading system attachment. Figure 25 shows the three hydraulic actuators, their load cells, and the whippletree arrangement used to apply equal loads to each of the test panel attachment cables. Each actuator was controlled by a closed-loop system that used load measurements indicated by a load cell as feedback. All three actuators were operated by a single programmed loading time history.

The simulation at a particular data event must include all significant environmental conditions beginning from some data reference. For strain gage loads measurements, the simulation must be started at the last available zero-load condition; for the X-15, this was just prior to B-52 takeoff. Thus, the wing simulation had to start at ambient conditions, cool down and cold soak to the launch condition, and then proceed to the X-15 flight heating profile.

A recirculating cooling system (Fig. 26) was constructed to provide the cool-down and cold-soak portion of the simulation. During a particular test, the cooler mixes ambient air with liquid nitrogen (LN_2), which evaporates and extracts the heat of vaporization from the ambient air, cooling it to the desired temperature. This air is then directed to the test specimen. The upper and lower IR heater reflectors were used as part of the cooling system enclosure.

Shuttle Elevon

A portion of the Space Shuttle outboard wing and a complete elevon were used as a test specimen for a series of combined heating and loading tests [4]. The primary purpose of these tests was to verify the functional capability of a system of seals between the wing and elevon. The test article is shown in Fig. 27. The wing box with attached elevon was cantilevered from a support structure. The superalloy flipper doors covering the cavity between the wing box and the elevon can be seen. Hydraulic actuators, above and below the test article, applied loads to the structure through aluminum load pads. The load pads were bonded to the structure with silicone rubber. All loads were applied to portions of the structure which were normally covered with thermal protection system (TPS) and, therefore, at temperatures less than 350 °F.

Figure 28 shows the complexity of the IR heater setup surrounding the shuttle elevon. The photograph was taken from the root end of the structure looking outboard. Actively cooled reflectors, shown in the upper center of the picture, were used to heat the superalloy doors to approximately 1500 °F. All the remaining skin surfaces were heated to less than 350 °F with polished aluminum reflectors. The reflector system, seen in the upper left of Fig. 28, was also required to move in later tests to accommodate rotation of the elevon surface.

The test article is shown in Fig. 29 during a test surrounded by a quartz lamp heating system. The hydraulic actuators above the wing box can be seen. The actuator load rods pass through holes in the heater system so that they can provide load during the heating tests. The brightest quartz lamps correspond to locations around the cavity and seal system where test temperatures were highest. Cavity pressurization was provided by high-pressure nitrogen gas bottles (seen in the background) and vacuum was provided by a vacuum pump located outside the building. An independent frame was used to support deflection measurement transducers.

YF-12 Airplane

A program was conducted to measure flight loads on a YF-12A airplane [5]. The program consisted of flight and laboratory tests. During the flight tests, temperatures throughout the structure of the airframe were recorded concurrently with strain gage bridge measurements on the wing, fuselage, and control surfaces. The laboratory tests had two parts. First, a loading calibration of the strain gage bridges was performed. Second, thermal calibrations (discussed in the following paragraphs) were performed which simulated the measured skin and structural temperature profiles of flights at Mach 2.5, 2.75, and 3.0. The heating

control performance during the Mach 3 simulation was excellent, with a control error standard deviation for all channels of 5.6 °F. The temperatures resulting from the heating tests were compared with many flight measurements throughout the aircraft. Those comparisons showed the simulation of temperatures on the substructure thermocouples at strain gage locations to be good.

The YF-12A airplane has a total surface area of approximately 5000 ft^2. Since the safety aspects of the heating made quick access to the airplane necessary, the heater support structure was divided into sections, as shown in Fig. 30. There were two forebody sections, one for the left side and one for the right; four central heaters, a top and a bottom heater on each side; and a rear heater that covered top and bottom on both sides. The forebody sections and the lower central sections were mounted on V-grooved wheels that ran on inverted angle track and retracted sideways. To clear the nacelles, the inboard ends of the lower central sections had to be lowered by hydraulic jacks built into the frames, to a position near the floor before retraction. Separate main wheel well heaters were built to allow the lower central heaters to be retracted independently. The upper central sections were supported by towers and guy cables. Each section was counterbalanced about a hinge point at the towers and retracted upward. The rear section was mounted on V-grooved wheels and retracted rearward. The purpose of using V-grooved wheels and angle track was to make sure that the sections would return to their original position after being retracted, making it unnecessary to readjust the reflectors. Stops were permanently fastened to the tracks as an additional measure to insure proper positioning. The guy cables served a similar purpose for the upper central sections.

Figure 31 is an overhead view of the immense IR heater system and all of the electrical wiring. The reflectors for the heaters were made of type 310 stainless-steel sheets that were 0.075-in. thick. The sheets were designed to fit the contour of the airplane 6 in. away from the skin surface. The only forming operations necessary to match the surface contours of the airplane were rolling and bending; however, to produce conical shapes the rolling operation had to be performed with different radii at each end of the panel. Gaps were left between each panel to allow for thermal expansion and to permit minor adjustments to be made after the panels were installed. The gap size, which was approximately 0.5 in., was determined by assuming a panel temperature of 900 °F and calculating the amount of growth from the coefficient of thermal expansion for the material. A total of 444 panels and 15,870 quartz lamps were used in this heater system, excluding the internal nacelle heater, which is discussed later.

The heater system is shown in Fig. 32 in the open or retracted position and the aircraft has been moved into position. Thermocouples used for temperature control of the heater system are shown attached to the outer skin surfaces of the aircraft. The entire vehicle was given a fresh coat of high-emissivity black paint during test preparations.

The overall zoning arrangement for the upper surface external heater is shown in Fig. 33. The heater was divided into 450 zones; half were located on the left side of the airplane, the other half were positioned at the identical location on the right side. Since the airplane is symmetrical, zones in identical positions on each side of the airplane required the same heat input. Consequently, control thermocouples were installed only on the left side of the airplane, and data from these thermocouples were used to compute the power required for the entire zone. For safety reasons, 29 monitor thermocouples were located on the right side of the airplane at selected locations. A typical zone contained 24 12-in. lamps and 8 18-in. lamps and covered an area of approximately 12 ft^2. The power required for the total heating system with all zones operating at full power was estimated to be 18 MW.

An internal nacelle heater (Fig. 34) was designed and fabricated to account for the effects of structural heating from the left-hand engine. The heater was constructed of 20 stainless-steel panels that were rolled to form a cylinder 42 in. in diameter and 250-in. long. The panels were 0.075-in. thick. It was mounted on a monorail that was attached to the engine mounts inside the left nacelle. Retracting the nacelle heater required the retraction of the rear heater and the erection of a support structure so that the monorail could be extended outside the nacelle. A total of 560 quartz lamps were divided into 20 zones of equal size; 10 zones on the inboard side of the nacelle and 10 zones on the outboard side. Including the internal nacelle heater, the entire IR heater system consisted of 464 reflector panels, 16,430 quartz lamps, and 470 control zones which were each programmed to follow a designated temperature–time history. Although the system was capable of delivering over 18 MW of power, the maximum power used for a Mach 3 flight simulation was 3.5 MW. The relatively low power usage was primarily the result of a much higher heater efficiency than design calculation indicated.

The support of any test article being subjected to a thermal test is important, and the YF-12 airplane was no exception. To minimize thermal stresses, the right main gear was fixed, and the forward and left main gear were placed on ball transfer plates as shown in Figs. 35 and 36, respectively. The left main gear was free to move with the expansion of the airplane. The forward gear was permitted to move only forward and aft to relieve forces caused by longitudinal expansion.

In addition to the good simulation of the flight measured temperatures, it is significant to point out that the aircraft returned to flight status after these tests. Many research flights were conducted with the vehicle in subsequent years.

CONCLUDING REMARKS

Thermal testing of entire aerospace vehicles and structural components with infrared quartz heaters has been well established and widely used for several decades. The heaters are capable of accurately producing temperatures up to 3000 °F with heating rates up to 150 °F/sec and heat fluxes of 80 Btu/(ft^2-sec). It was shown during Mach 3 heating tests of the YF-12 airplane that control temperatures could be produced with standard deviations of 5.6 °F. Additionally, the thermal testing of the YF-12 proved that after the conclusion of such a test program, the airplane could be returned to active flight status.

There is a wide variety of quartz lamps and reflectors available that makes it relatively easy to tailor an infrared system for each unique test setup. Many variables enter into the system design such as lamp-to-lamp spacing, lamp to specimen distance, boundary conditions, combined heating–loading–cooling, surface emissivity, test article support, electrical power requirements, type of control, and heat flux variations (structurally and aerodynamically). Careful consideration of all details in the total system will help produce a successful thermal simulation.

REFERENCES

[1] Leger, Kenneth B., "High Temperature Test Methods Modular Graphite Heater Development," AFWAL-TM-88-168, 1988.

[2] Ripley, E.L., "Structural Tests for the Supersonic Transport Aircraft," Royal Aircraft Establishment, Technical Report 70121, 1970.

[3] DeAngelis, V. Michael and Roger A. Fields, *Techniques for Hot Structures Testing*, NASA TM-101727, 1990.

[4] *Workshop on Correlation of Hot Structures Test Data and Analysis*, NASA CP-3065, 1990, Vol. 1, pp. 117, 133, and 279; and Vol. 2, pp. 118, 203, and 238.

[5] NASA YF-12 Flight Loads Program, NASA TM-X-3061, 1974.

[6] Fields, Roger A. and Andrew Vano, *Evaluation of an Infrared Heating Simulation of a Mach 4.63 Flight on an X-15 Horizontal Stabilizer*, NASA TN D-5403, 1969.

[7] Sefic, Walter J., *NASA Dryden Flight Loads Research Facility*, NASA TM-81368, 1981.

[8] Zamanzadeh, Behzad, William F. Trover, and Karl F. Anderson, "DACSII-A Distributed Thermal/Mechanical Loads Data Acquisition and Control System," International Telemetering Conference/'87, Instrument Society of America, San Diego, CA, July 15, 1987.

[9] Fields, Roger A., *Thermal Testing at NASA Ames-Dryden*, Fourth National Aero Space Plane Technology Symposium, Feb. 17–19, Edwards, CA, Vol. 6, CP-4027, 1988.

[10] Fields, Roger A., Lawrence F. Reardon, and William H. Siegel, *Loading Tests of a Wing Structure for a Hypersonic Aircraft*, NASA TP-1596, 1980.

[11] Quinn, Robert D. and Roger A. Fields, *Comparison of Measured and Calculated Temperatures for a Mach 8 Hypersonic Wing Test Structure*, NASA TM-85918, 1986.

[12] Monaghan, Richard C. and Roger A. Fields, *Experiments to Study Strain-Gage Load Calibrations on a Wing Structure at Elevated Temperatures*, NASA TN D-7390, 1973.

[13] Fields, Roger A., Frank V. Olinger, and Richard C. Monaghan, *Experimental Investigation of Mach 3 Cruise Heating Simulations on a Representative Wing Structure for Flight-Loads Measurement*, NASA TN D-6749, 1972.

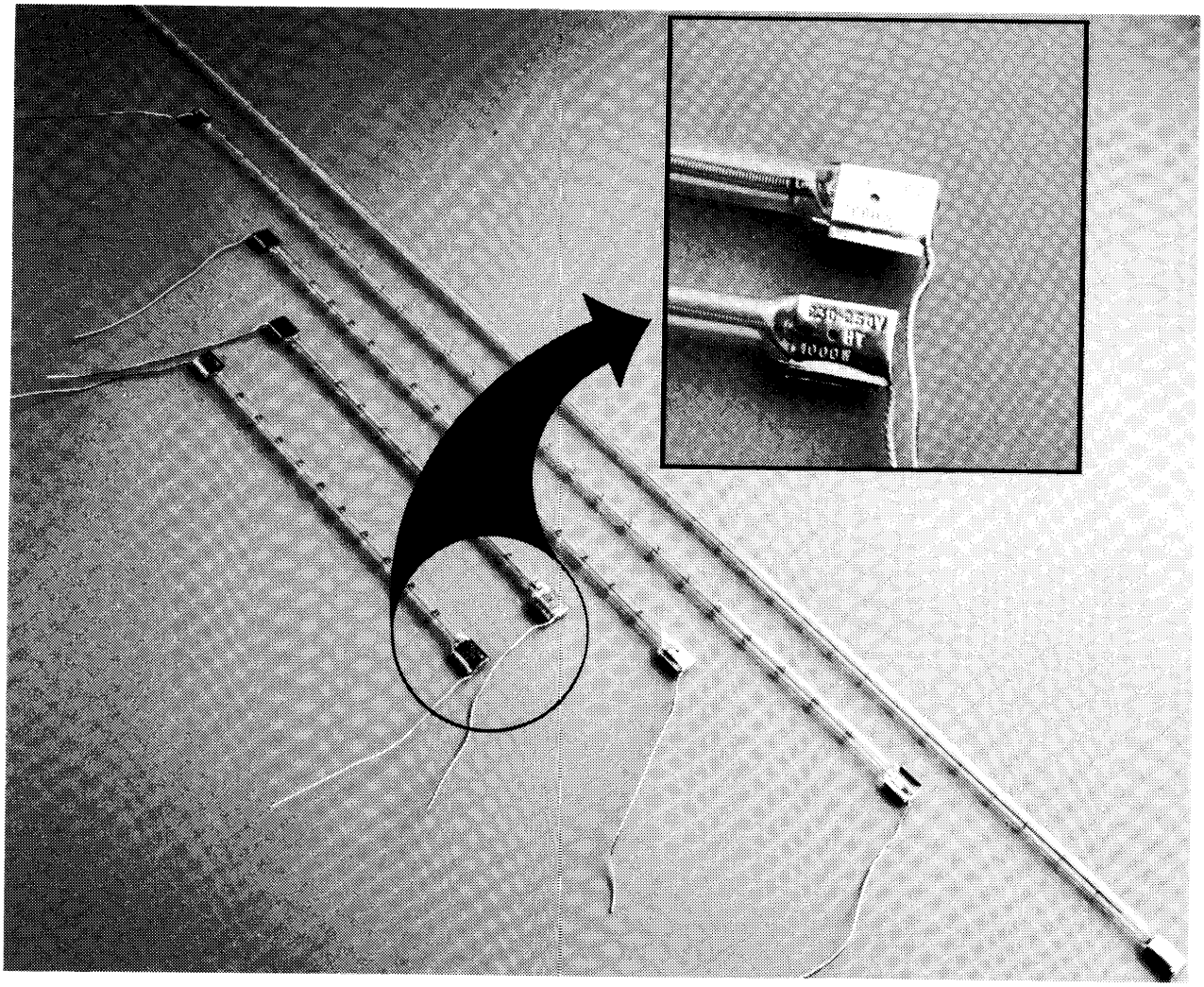

EC91 464-1

Fig. 1: Typical infrared quartz lamps

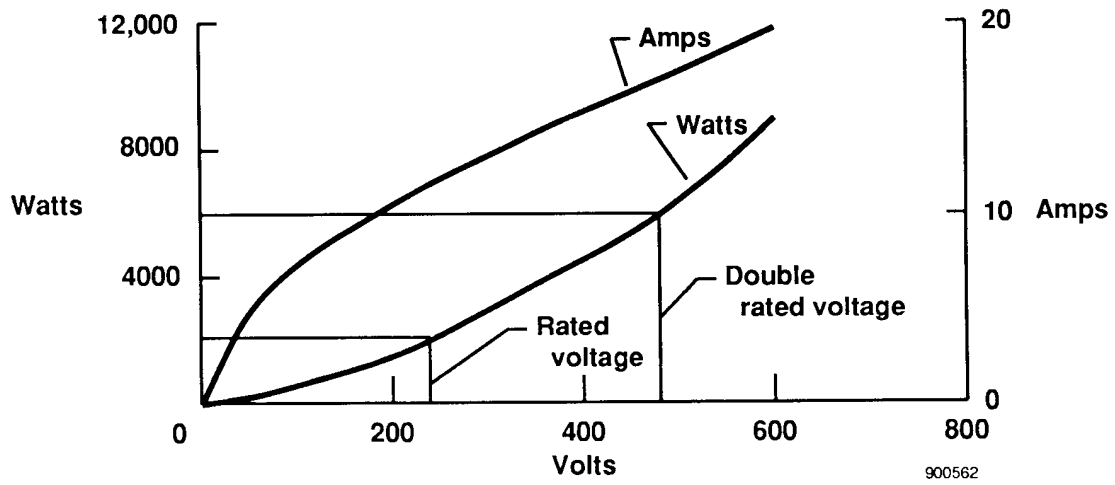

Fig. 2: Characteristics of 200 W/in., T-3, 10-in. quartz lamps

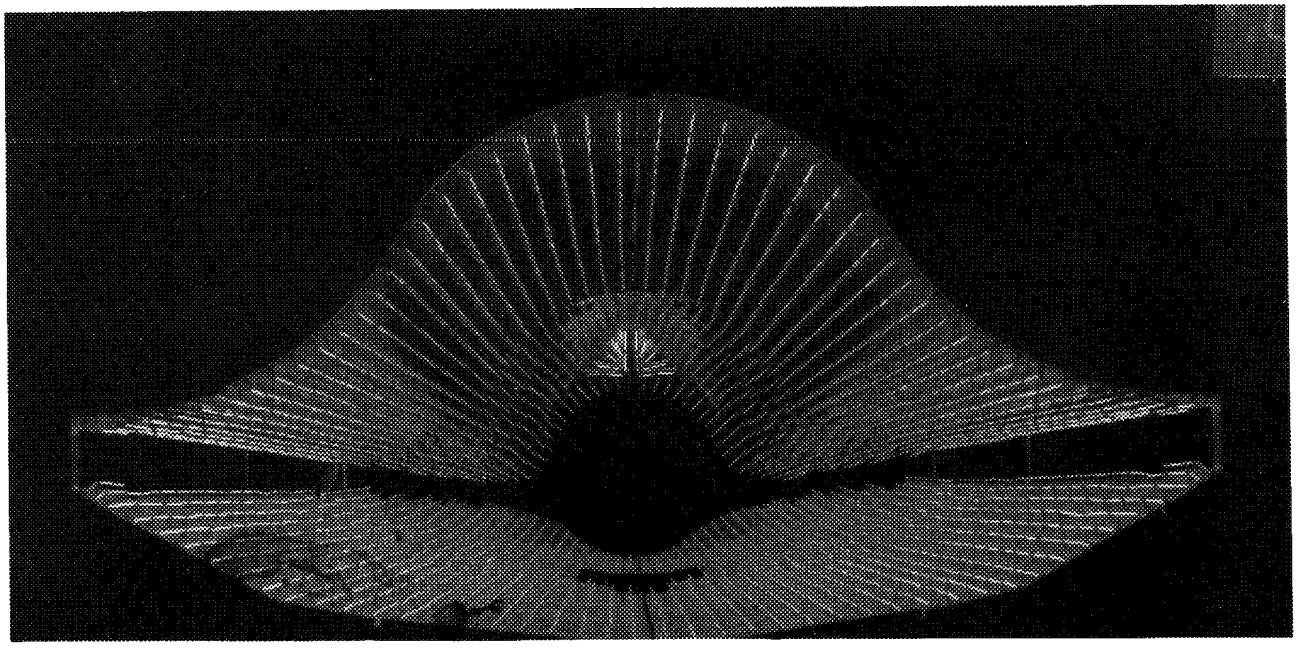

ECN 2789

Fig. 3: Polished stainless-steel reflectors for YF-12 forebody test

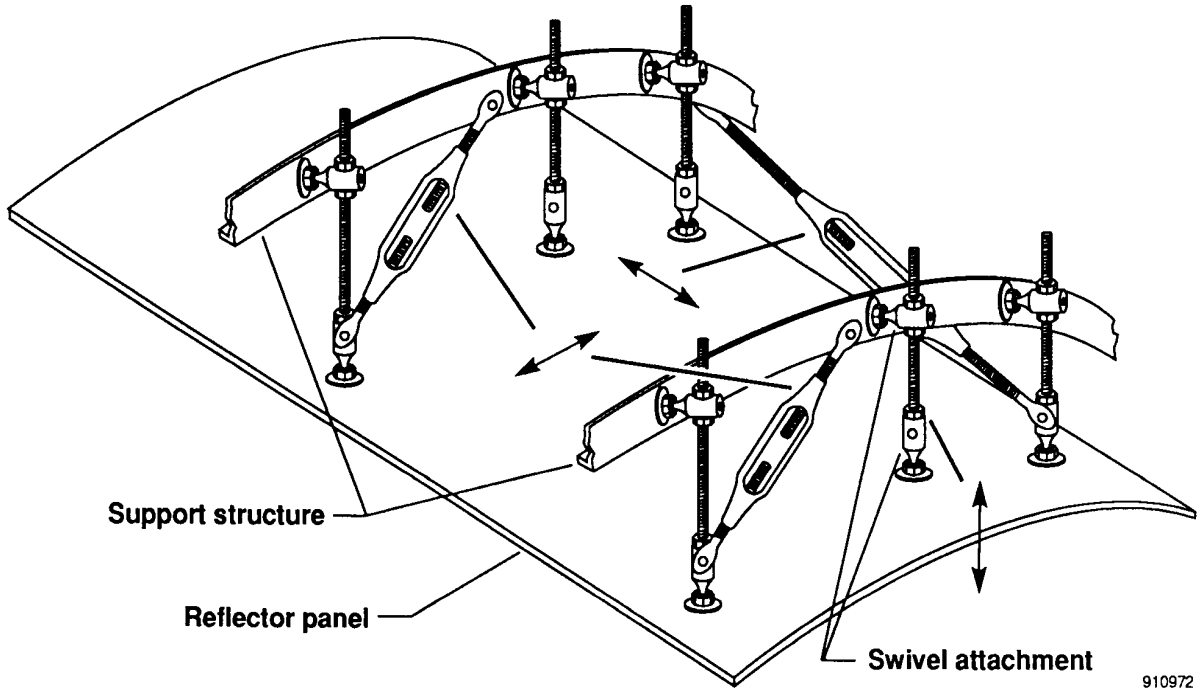

Fig. 4: Heater reflector panel attachment

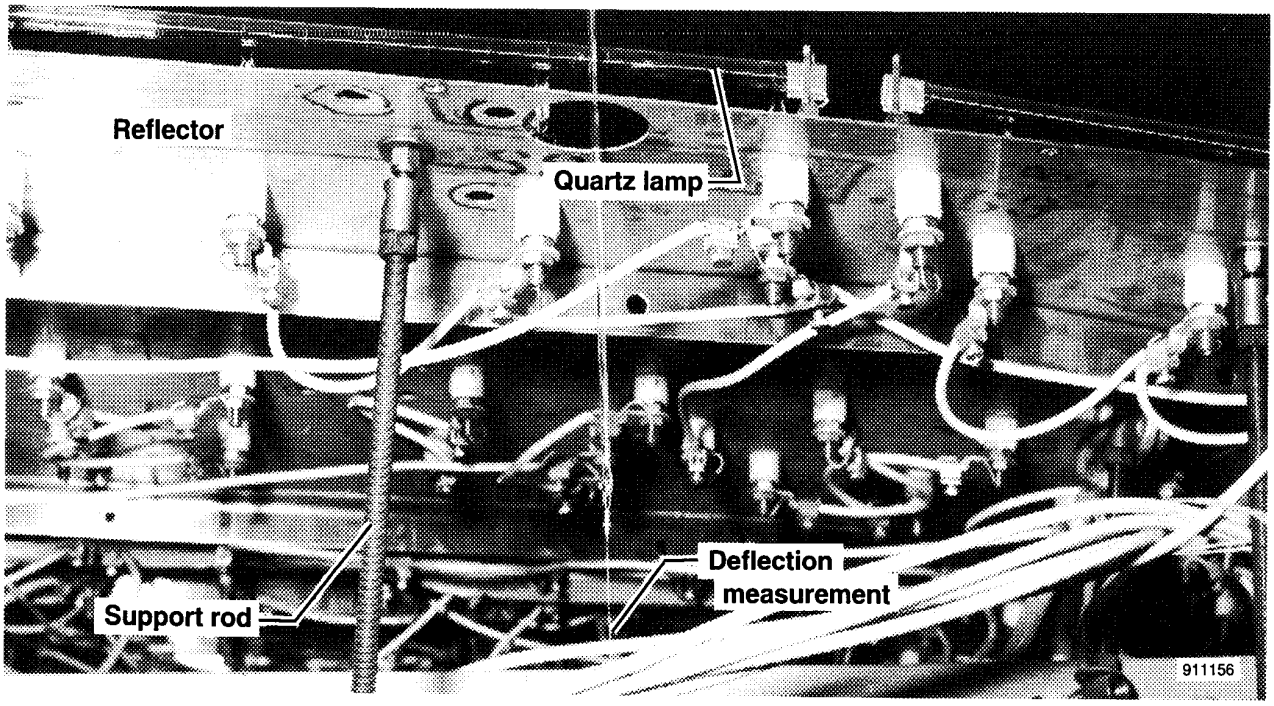

Fig. 5: Close up view of backside of stainless-steel reflector

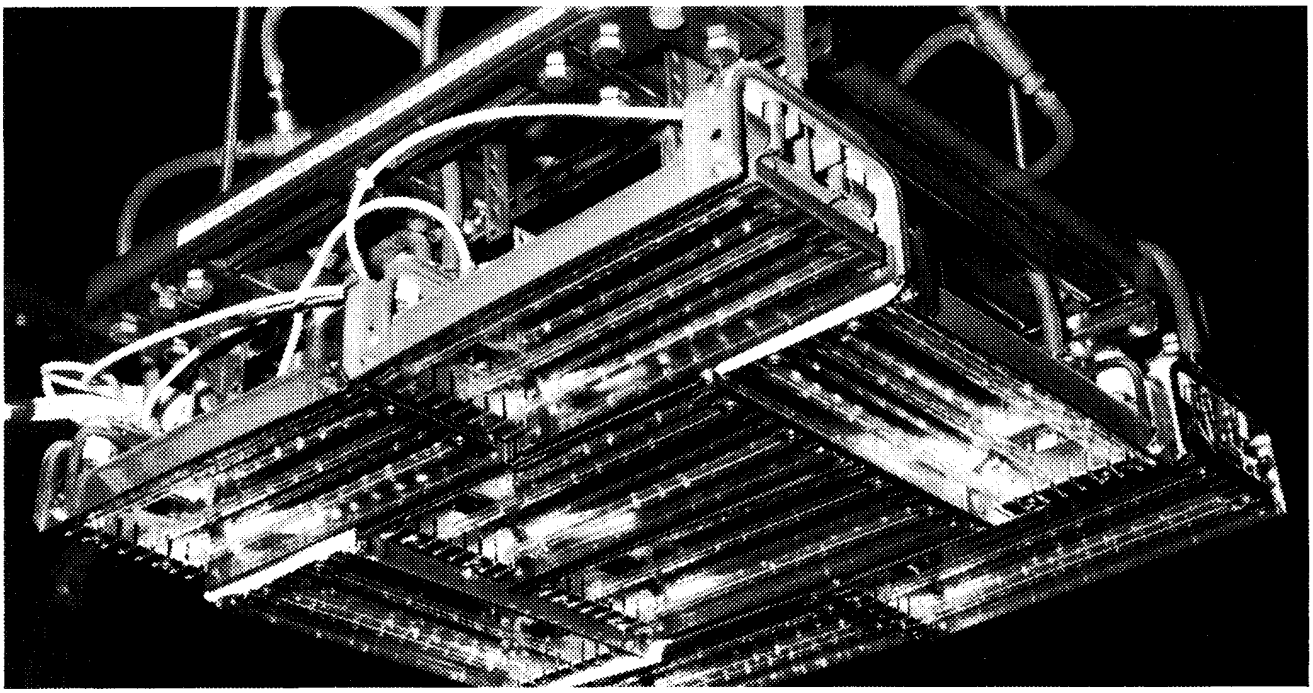

EC86 33504-009

Fig. 6: Gold plated stainless-steel reflector

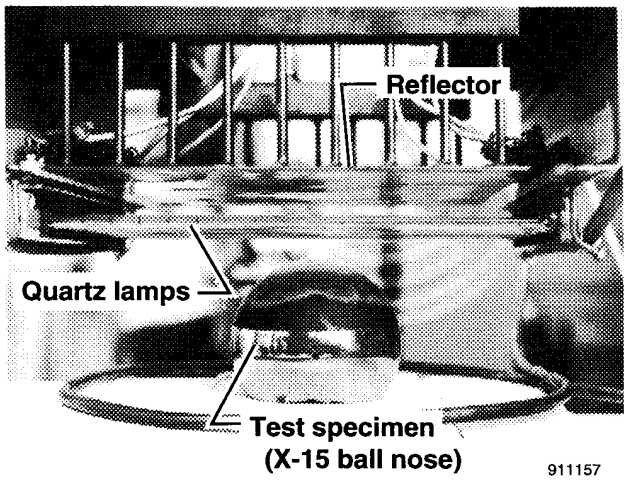

Fig. 7: Edge view of a water cooled polished aluminum reflector

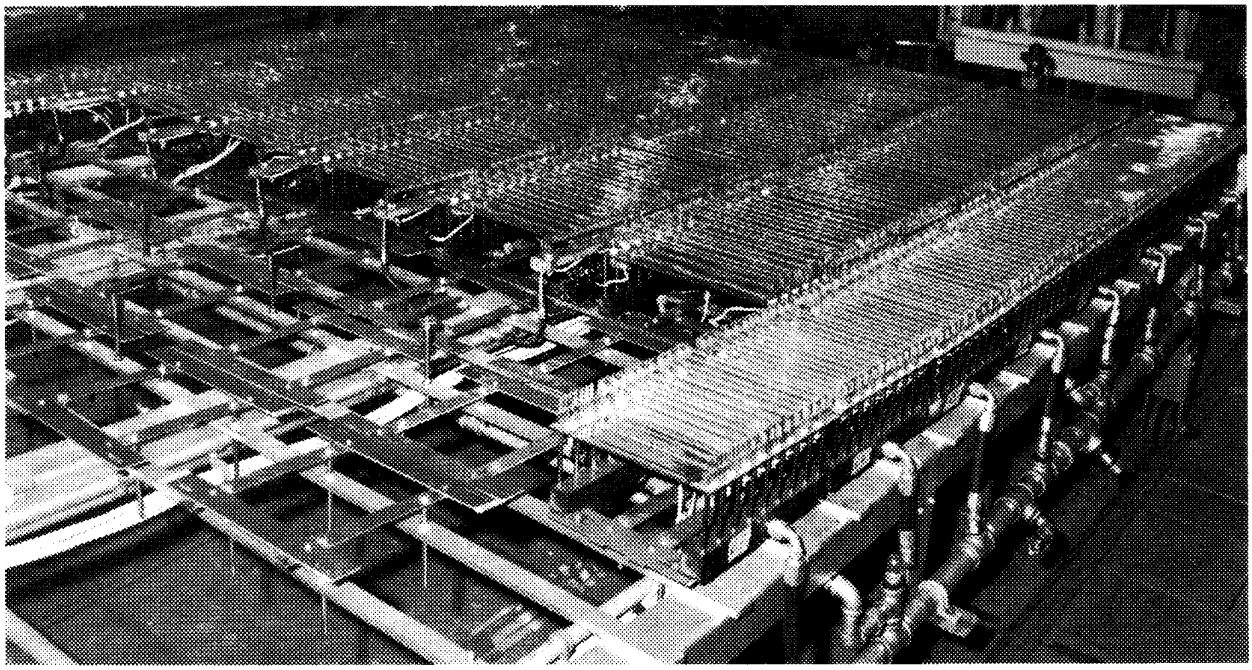

E 29937

Fig. 8: An array of water cooled polished aluminum reflectors

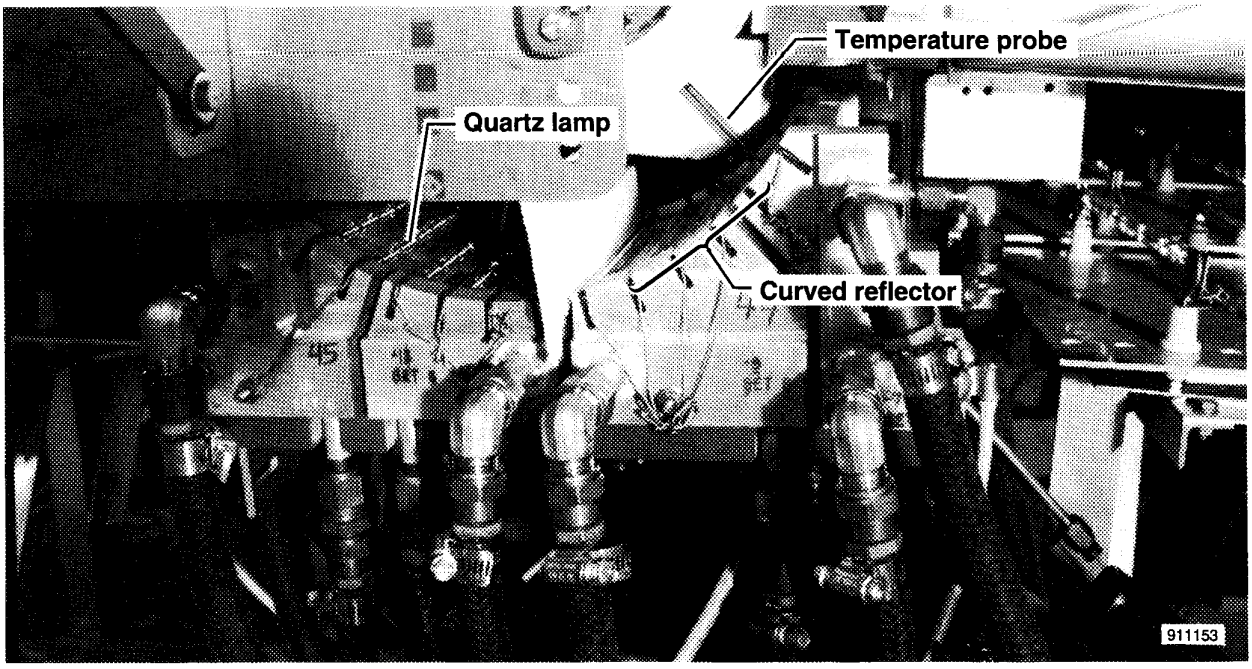

Fig. 9: Curved water cooled aluminum reflector

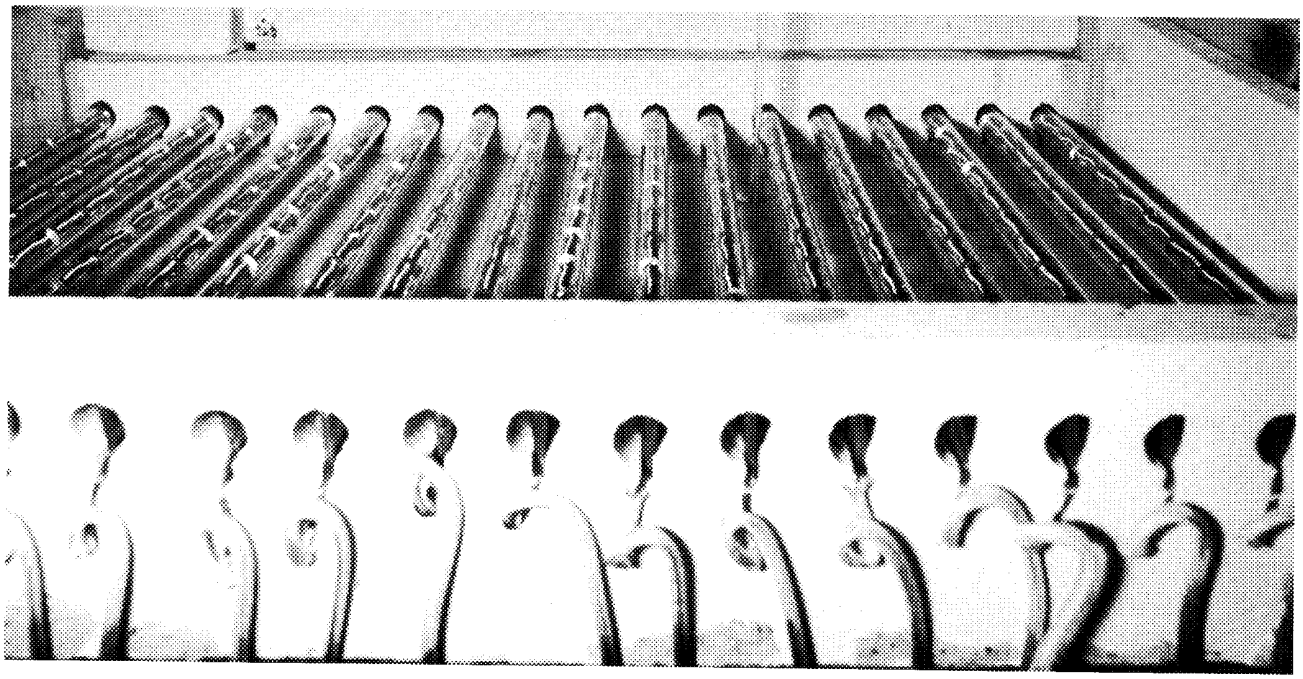

E 36733

Fig. 10: Ceramic reflector

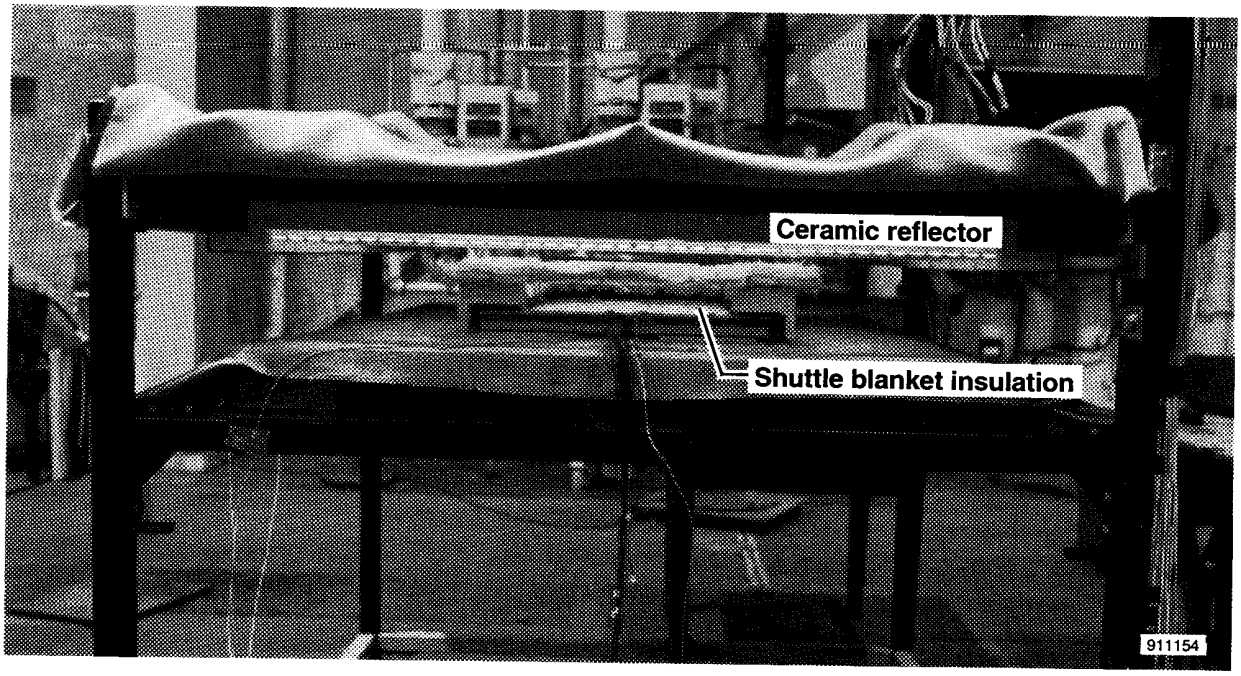

Fig. 11: Ceramic reflectors being used for shuttle insulation test

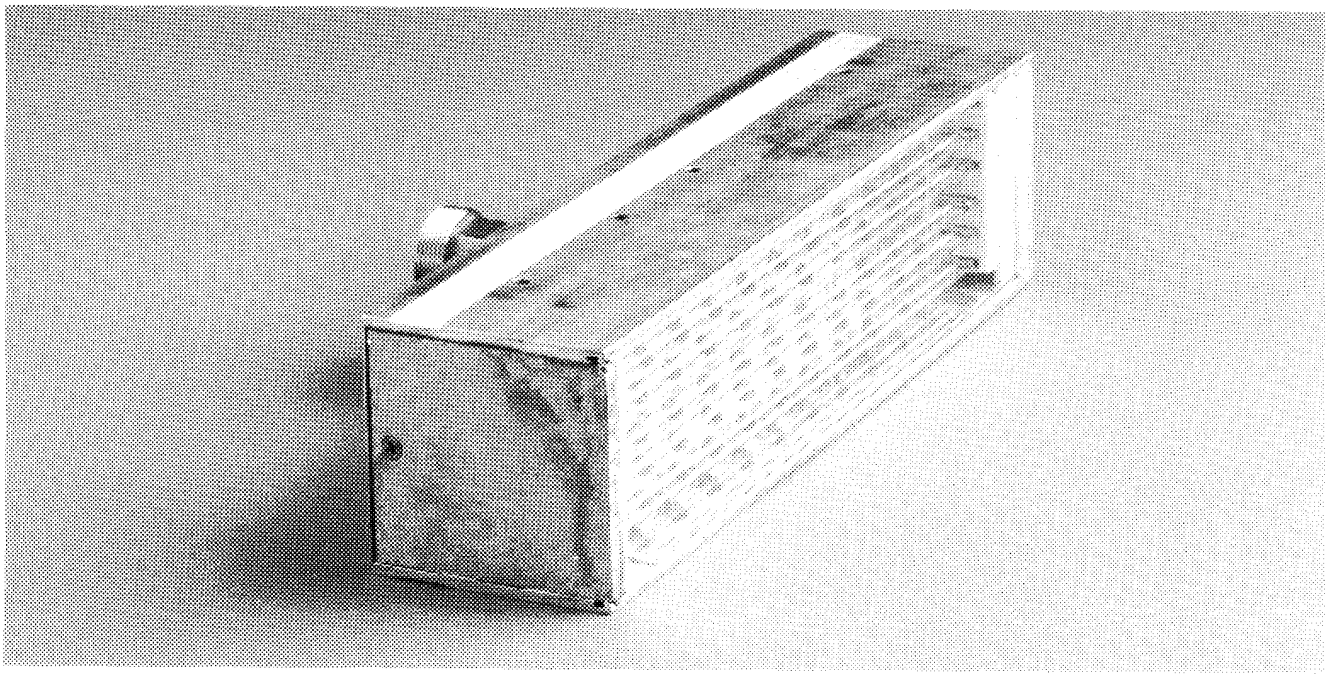

EC91 464-3

Fig. 12: Water and air cooled, polished aluminum heater unit

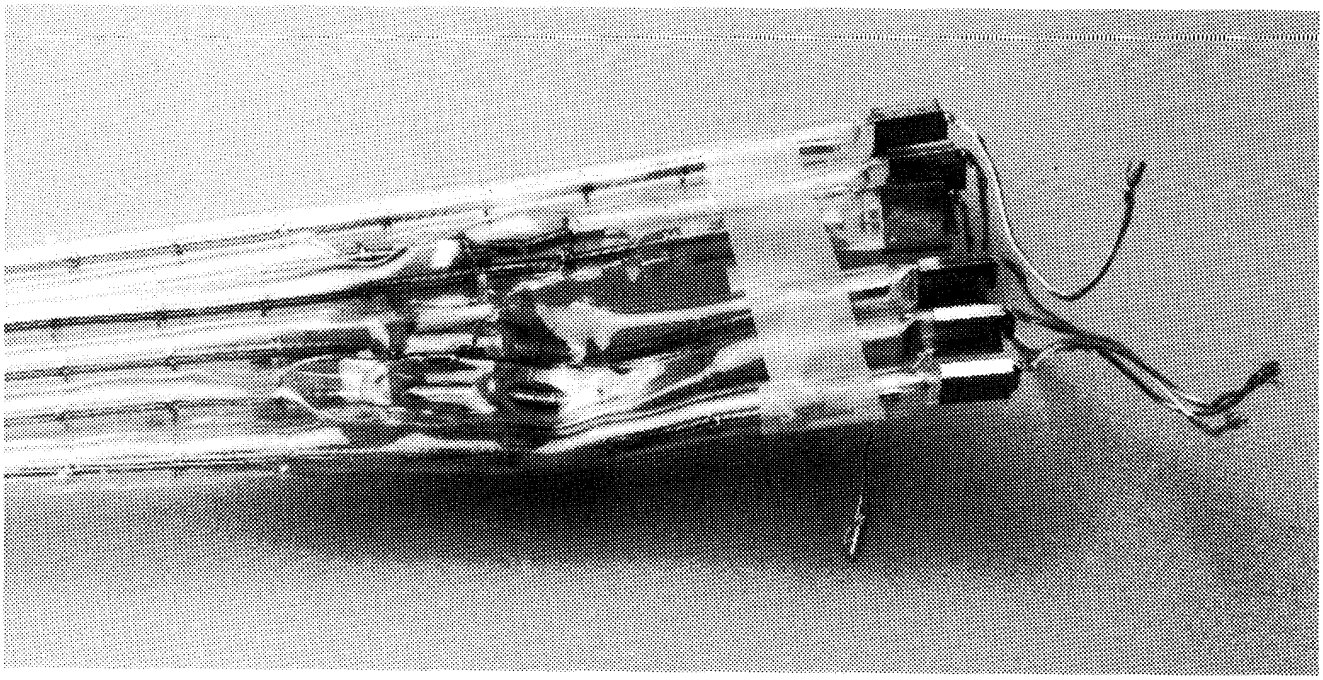

EC91 327-3

Fig. 13: Damaged quartz lamps

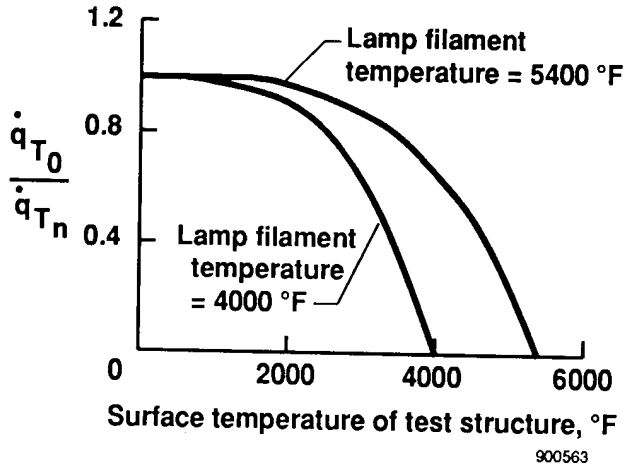

Fig. 14: Ratio of radiant heat flux

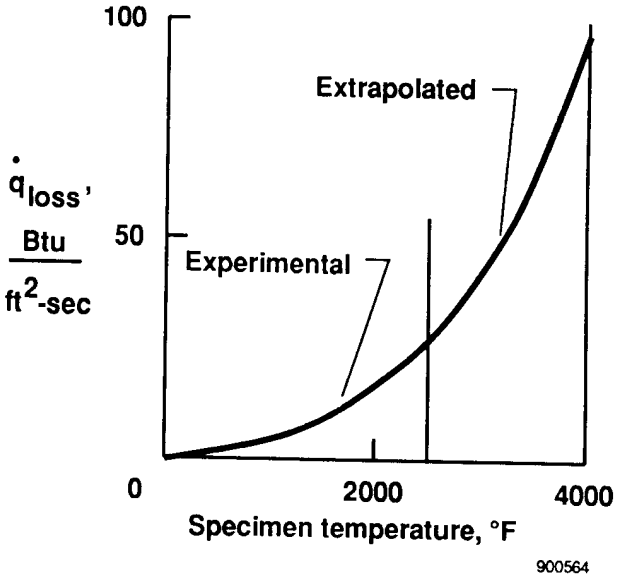

Fig. 15: Heat flux loss

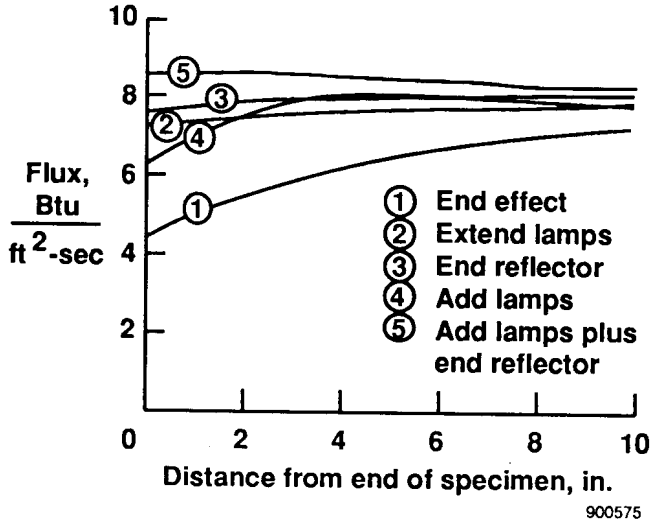

Fig. 16: Infrared heater end effects

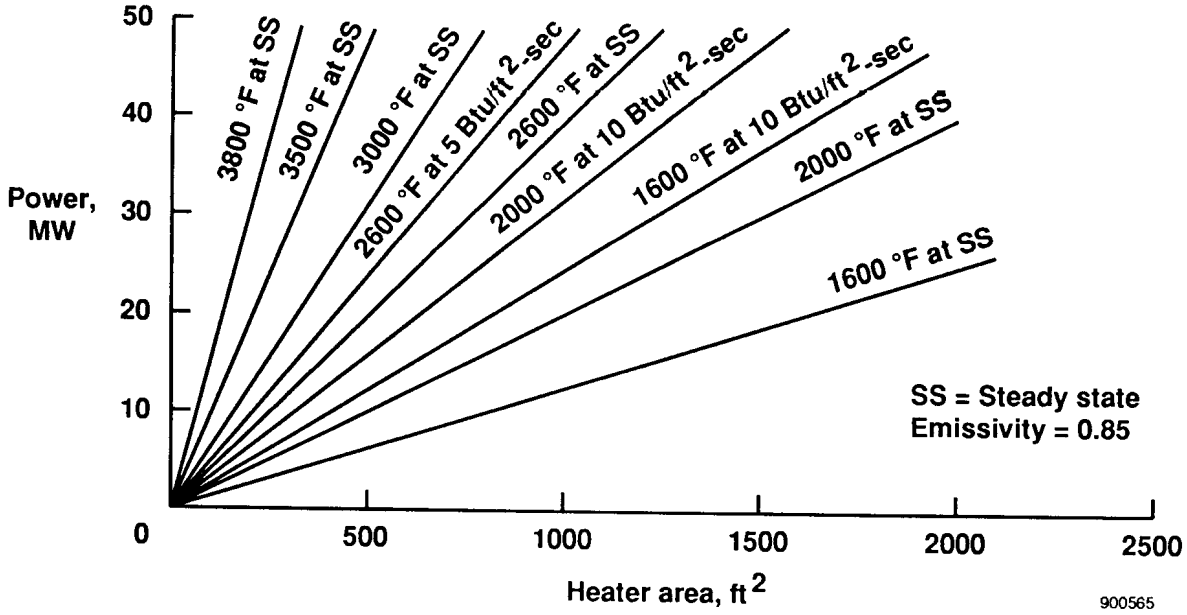

Fig. 17: Power required as a function of heater area

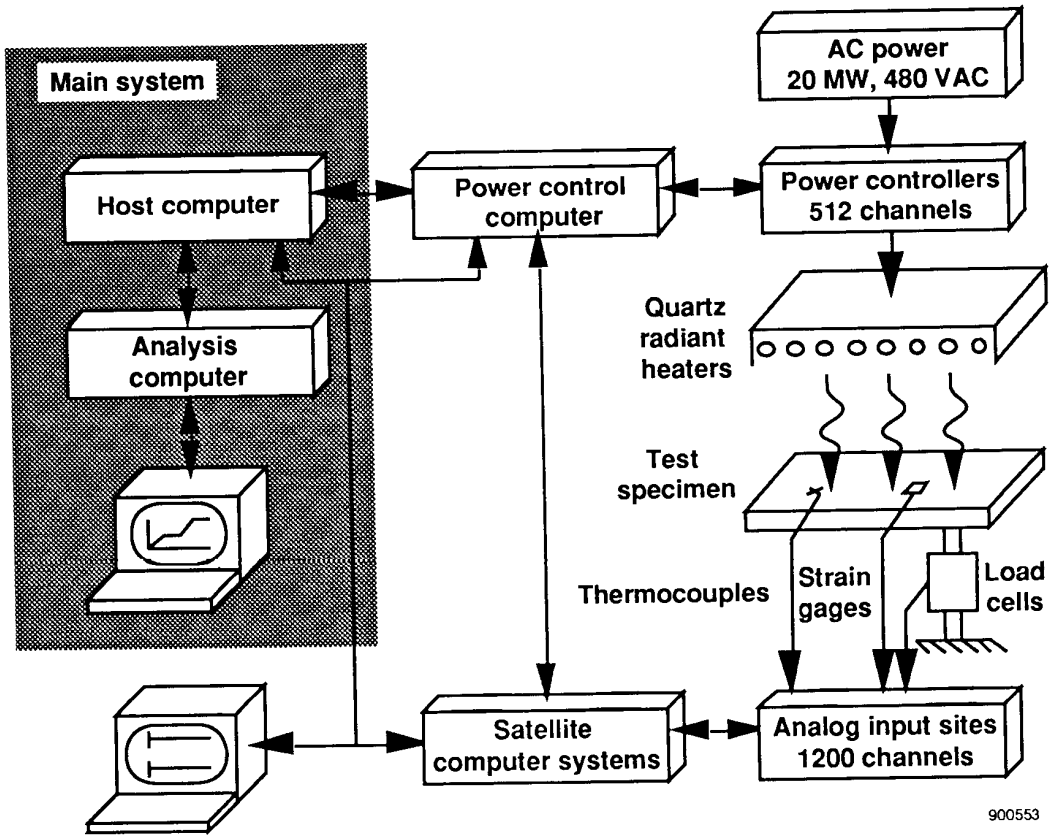

Fig. 18: Data acquisition and control system

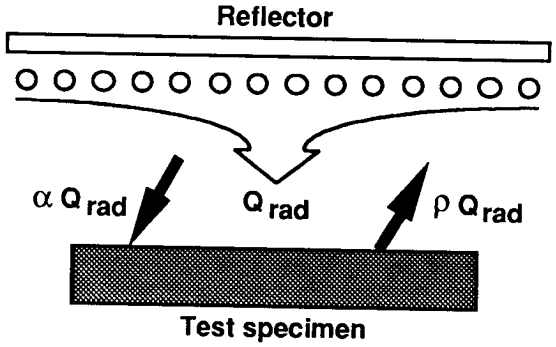

Q_{rad} = Total radiant heat flux from heater

ρ = Reflectivity

ρQ_{rad} = Heat reflected

ε (Emissivity) = α (Absorptivity)

$\alpha Q_{rad} = \varepsilon Q_{rad}$ = Heat absorbed by the test panel

Minimum power when $\varepsilon = 1$
Maximum power when $\rho = 1$

900577

Fig. 19: Effect of surface emissivity on power

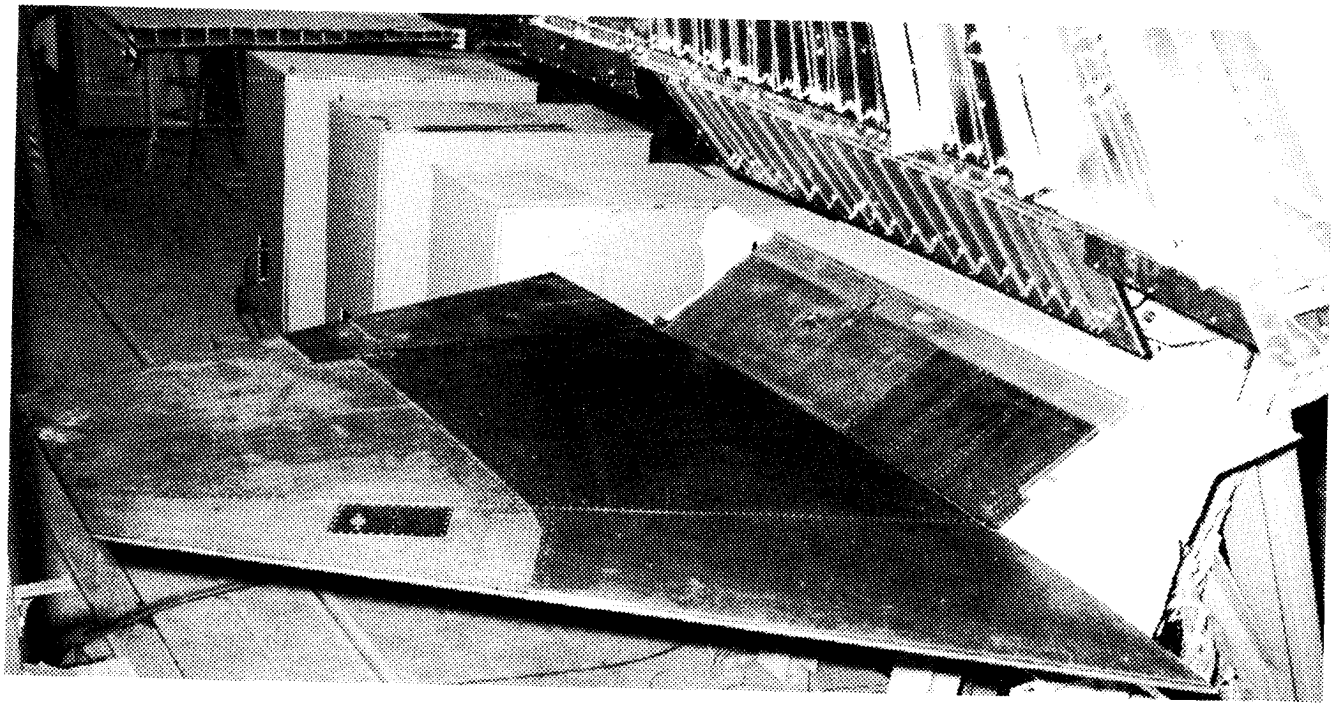

E-20336

Fig. 20: X-15 wing as removed from aircraft

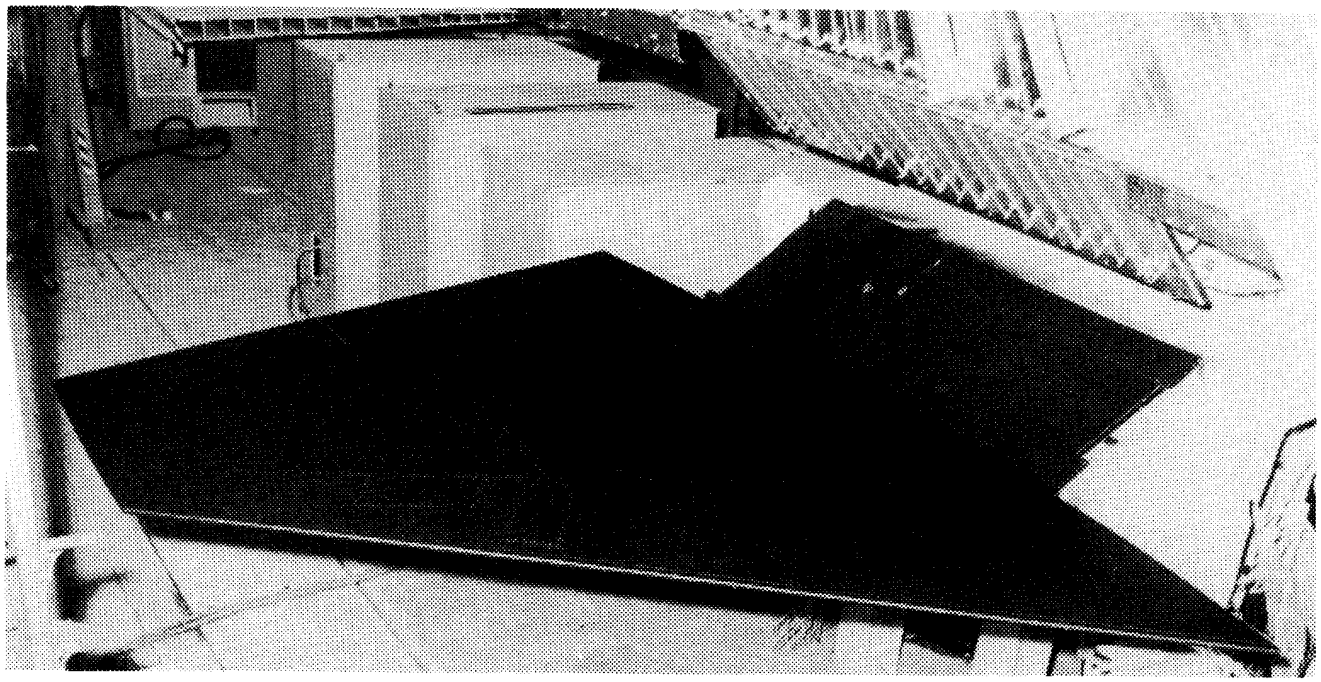

E-20338

Fig. 21: X-15 wing with high-emissivity paint

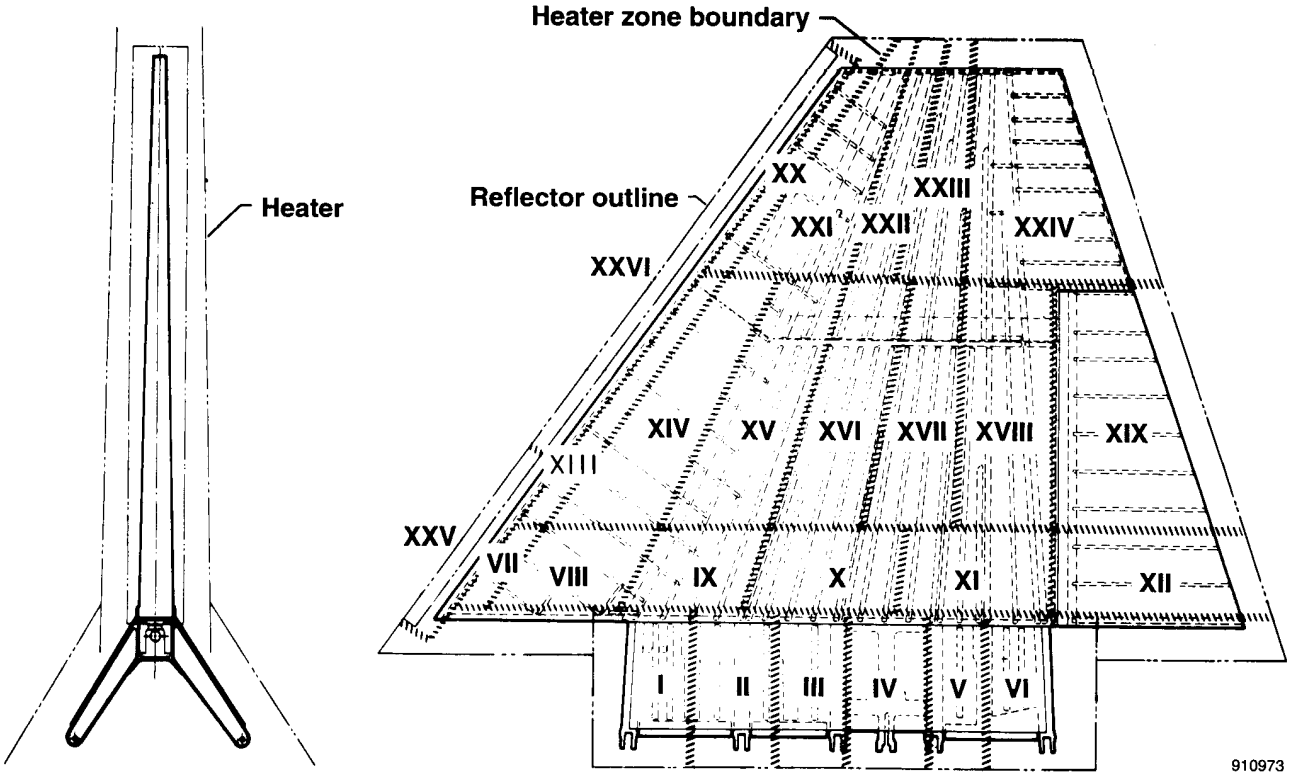

Fig. 22: Heater system zoning

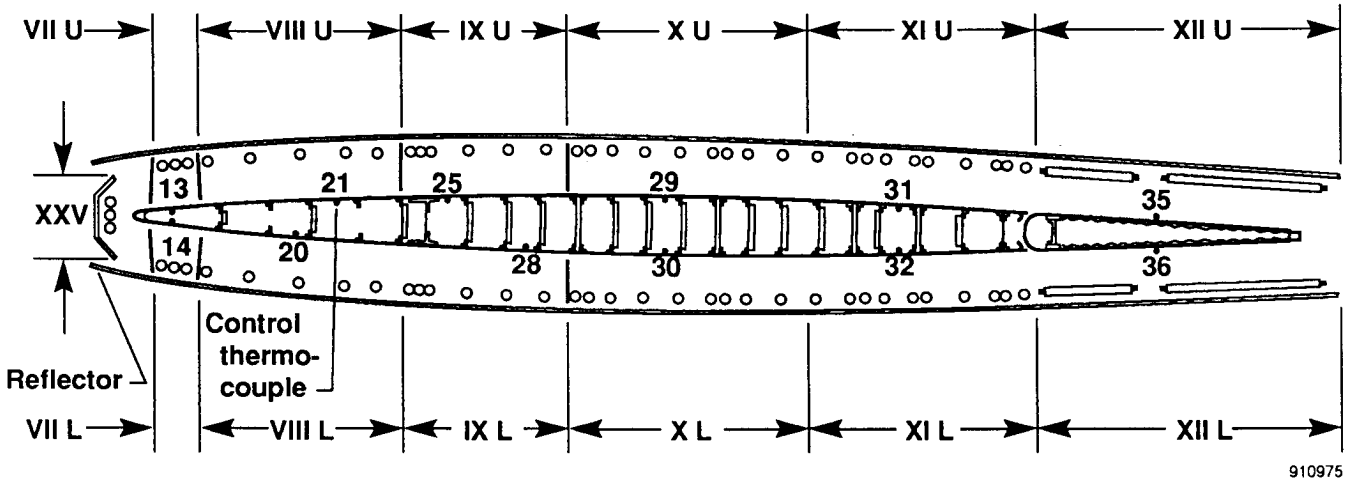

Fig. 23: Root station structure and heater

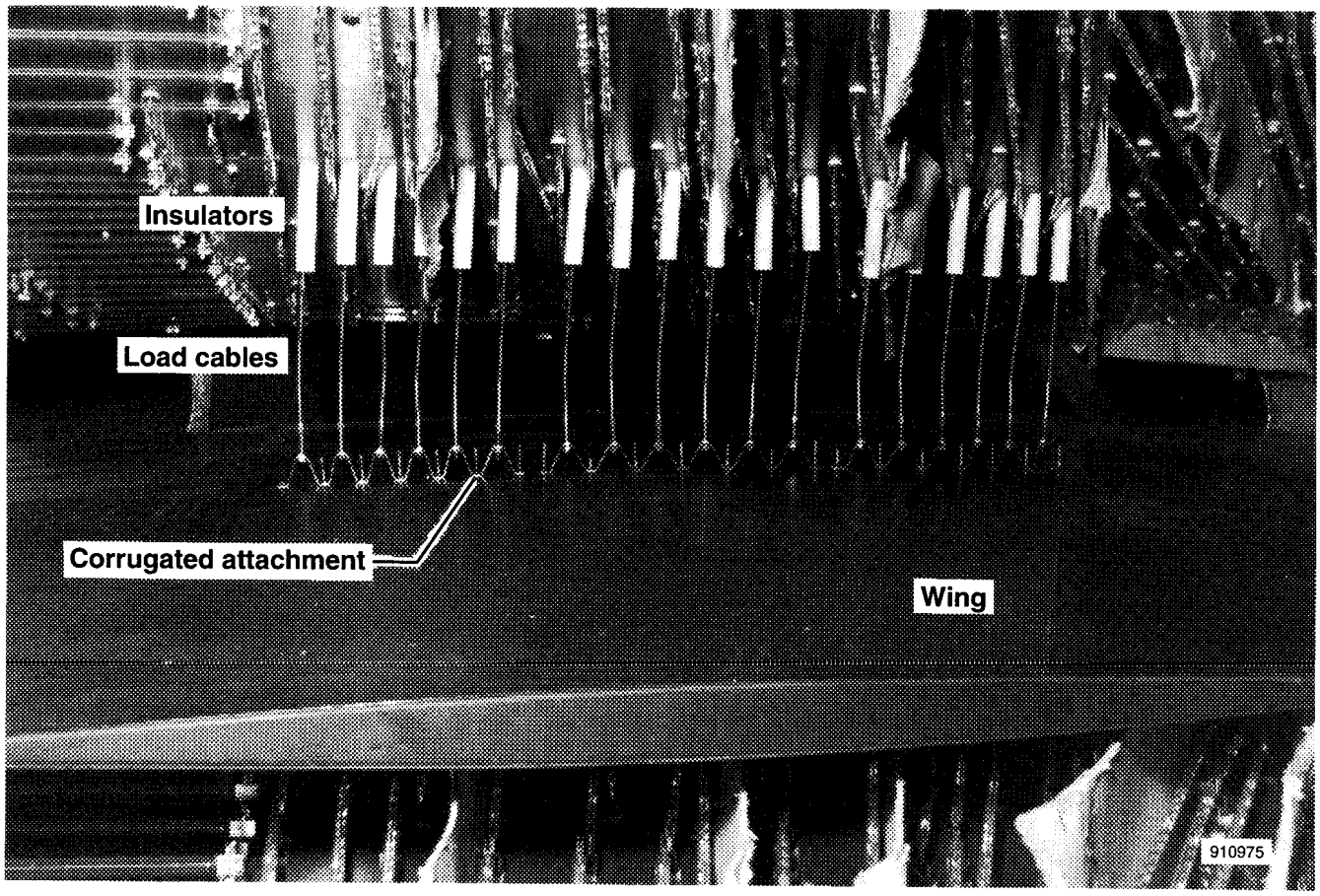

Fig. 24: Wing loading attachment

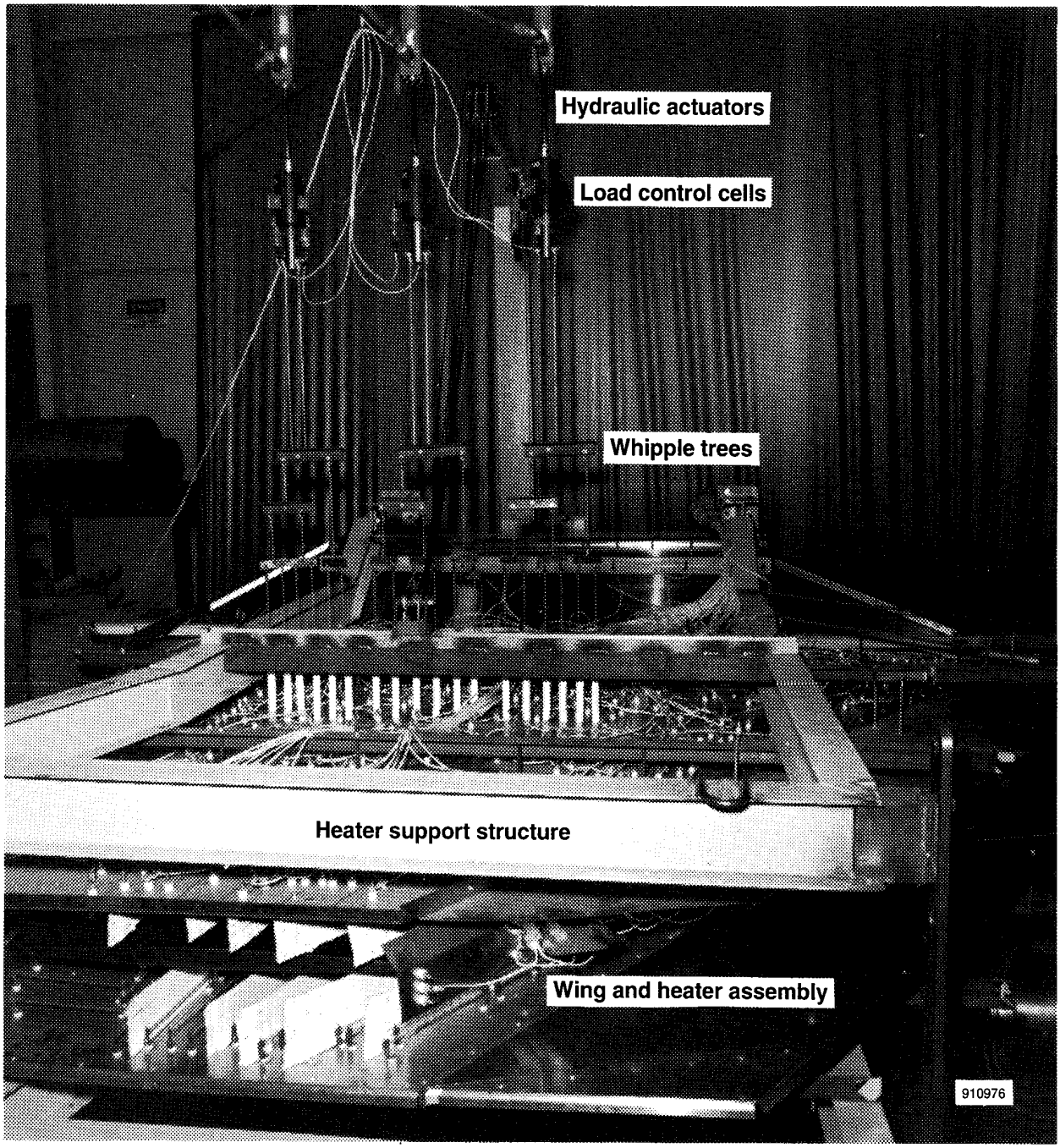

Fig. 25: Combined heating and loading test setup

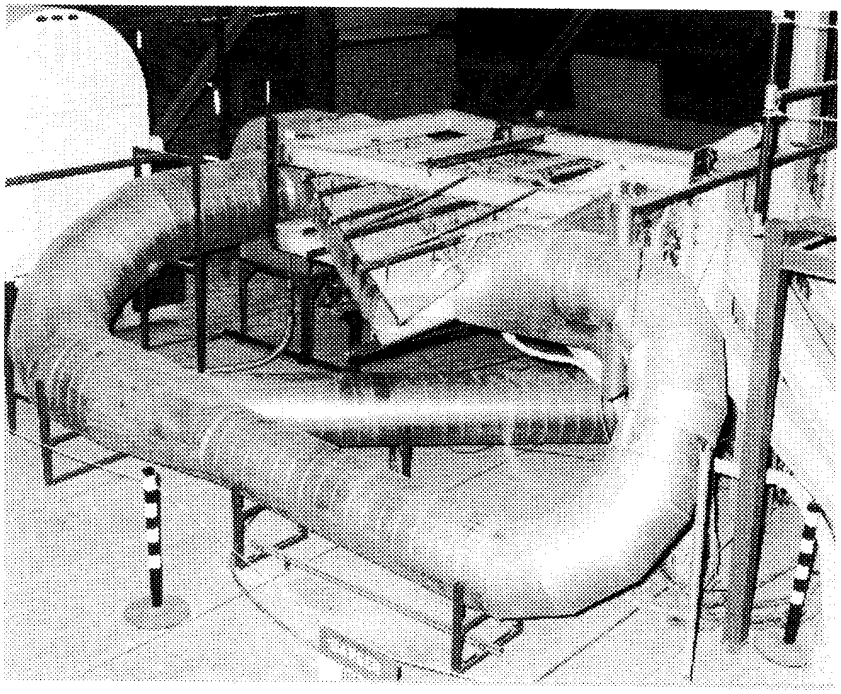

E-21634

Fig. 26: Combined cooling and heating system

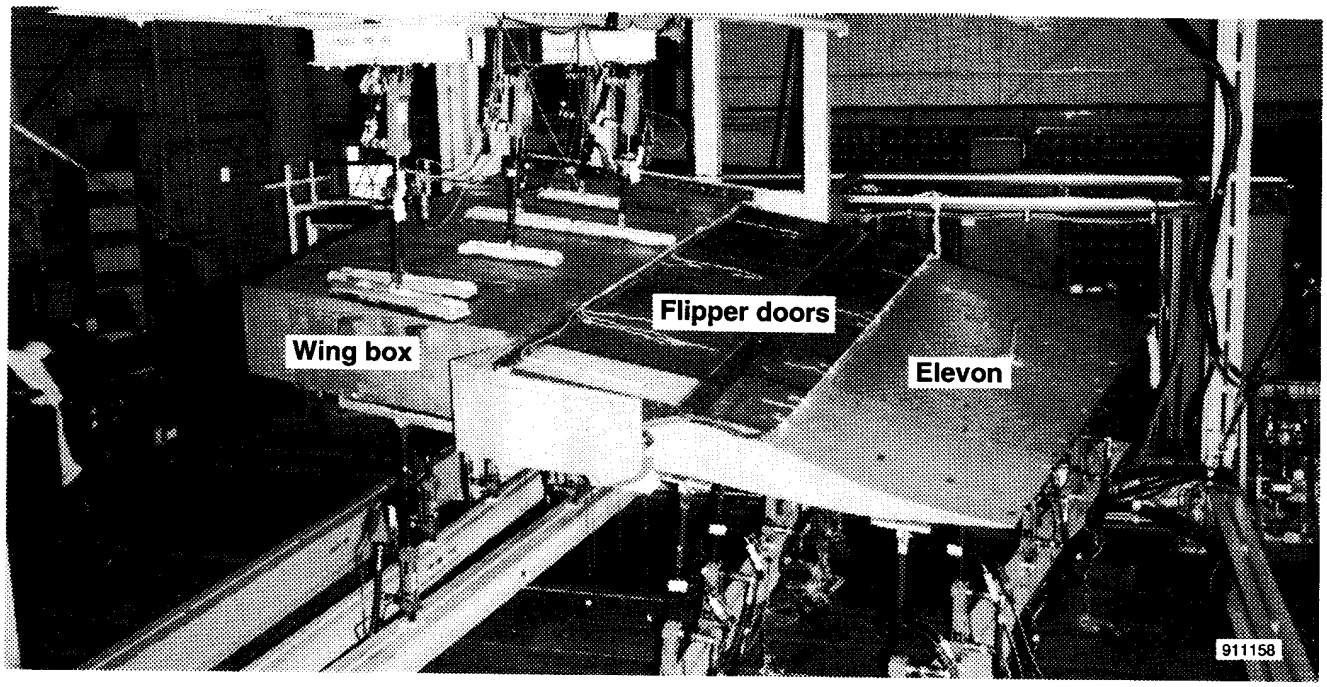

Fig. 27: Shuttle wing—elevon loading test setup

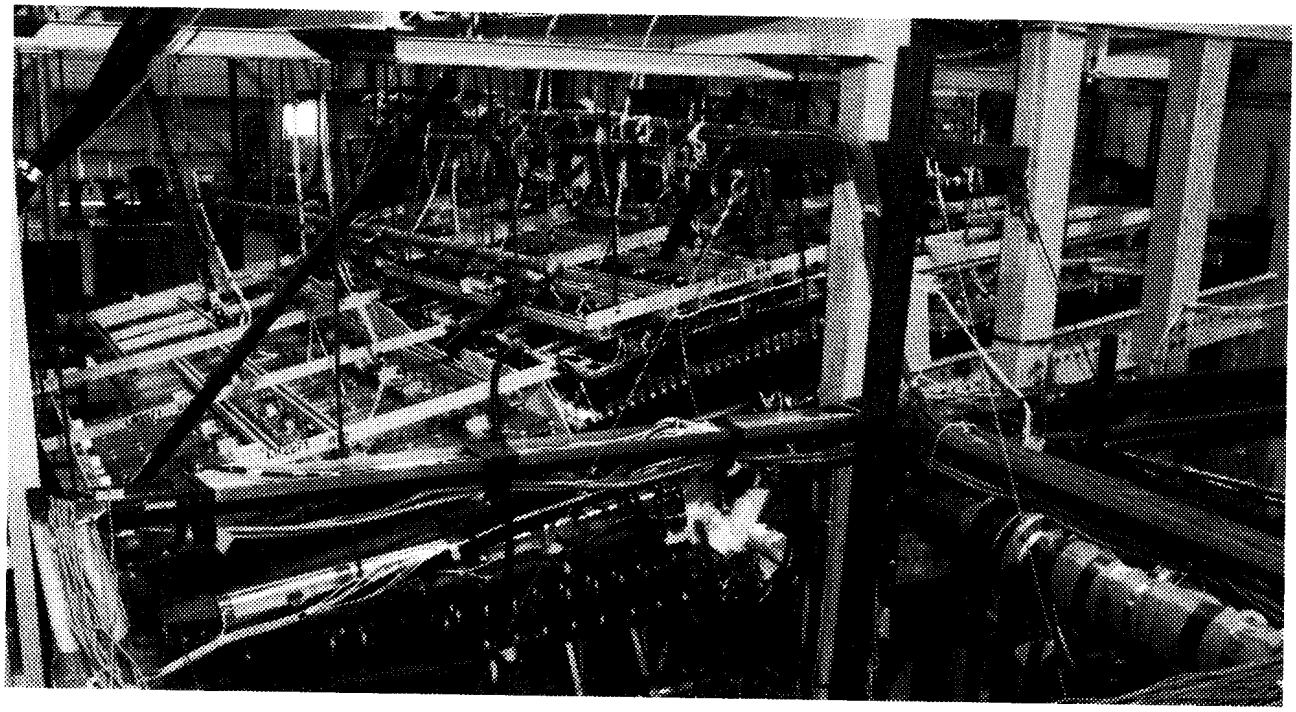

ECN 11279

Fig. 28: Shuttle wing—elevon heating system

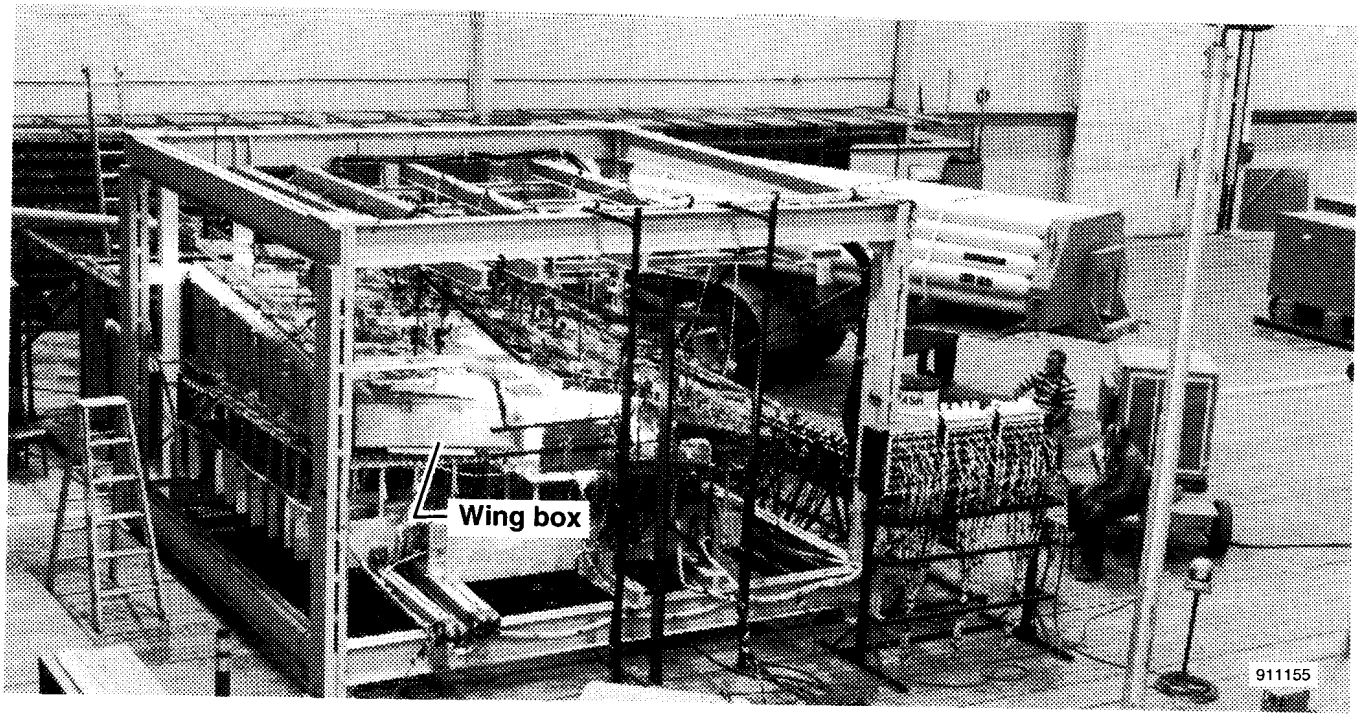

Fig. 29: Shuttle wing—elevon combined heating and loading test

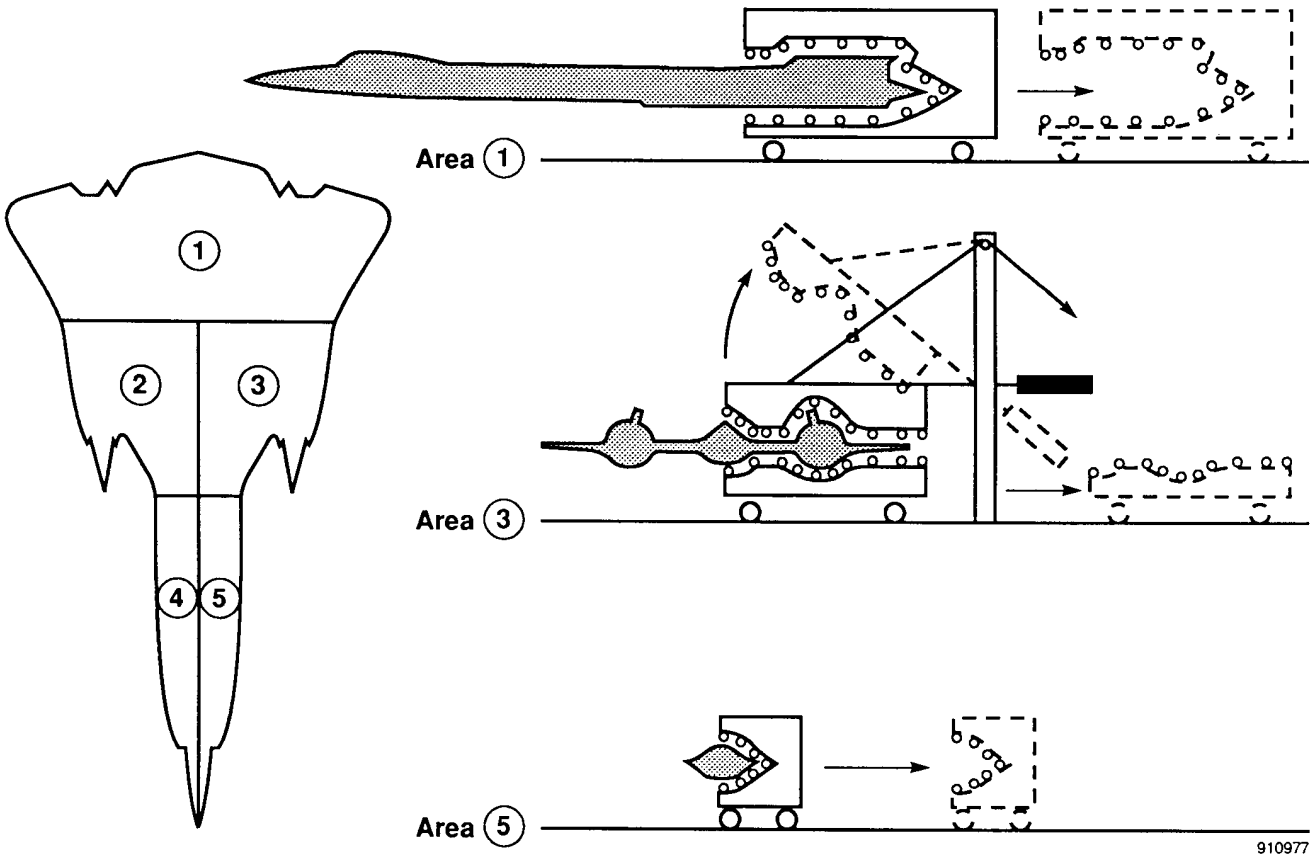

Fig. 30: YF-12 infrared heater panel configuration

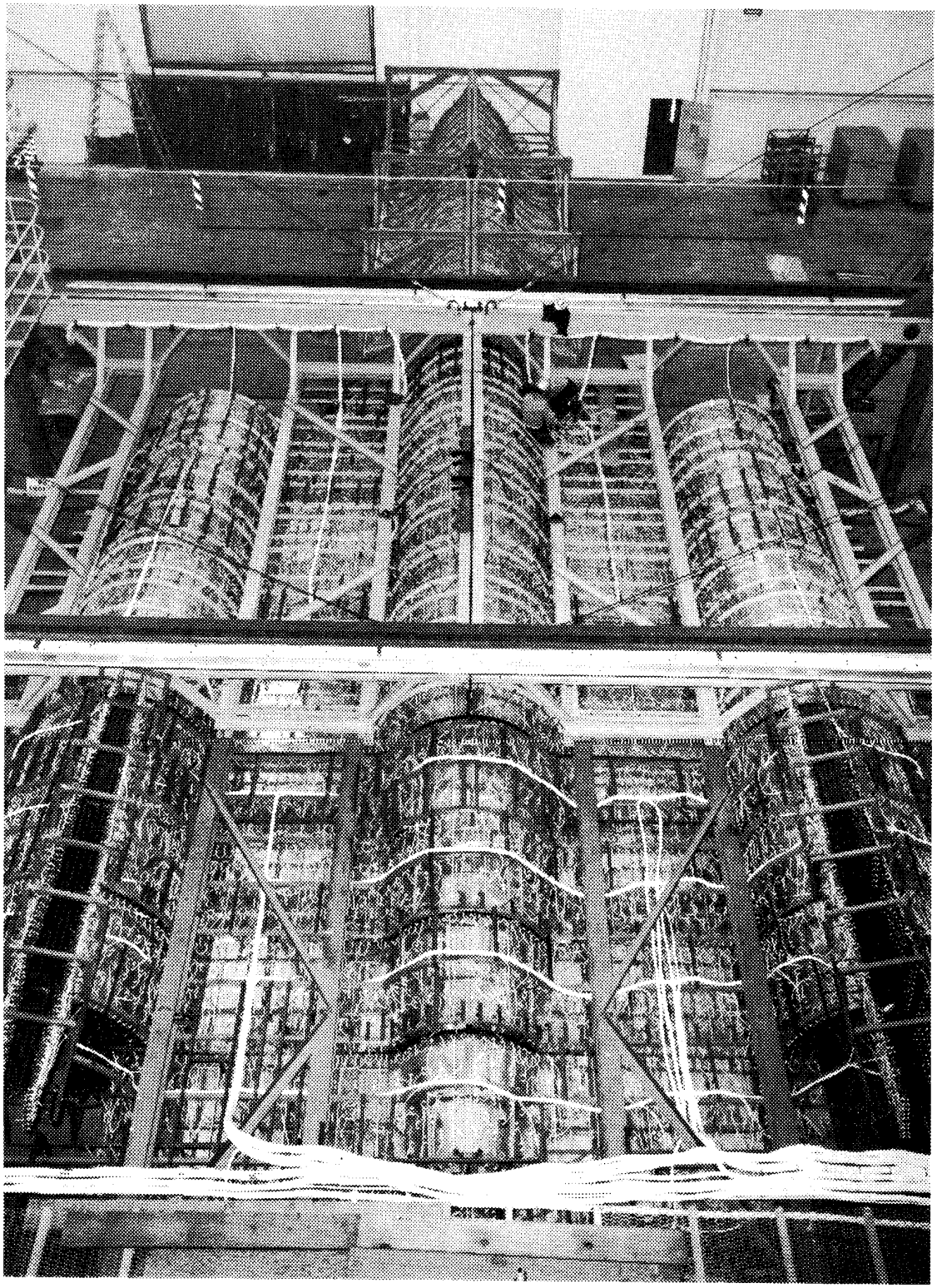

E-24098

Fig. 31: Overhead view of YF-12 heater system

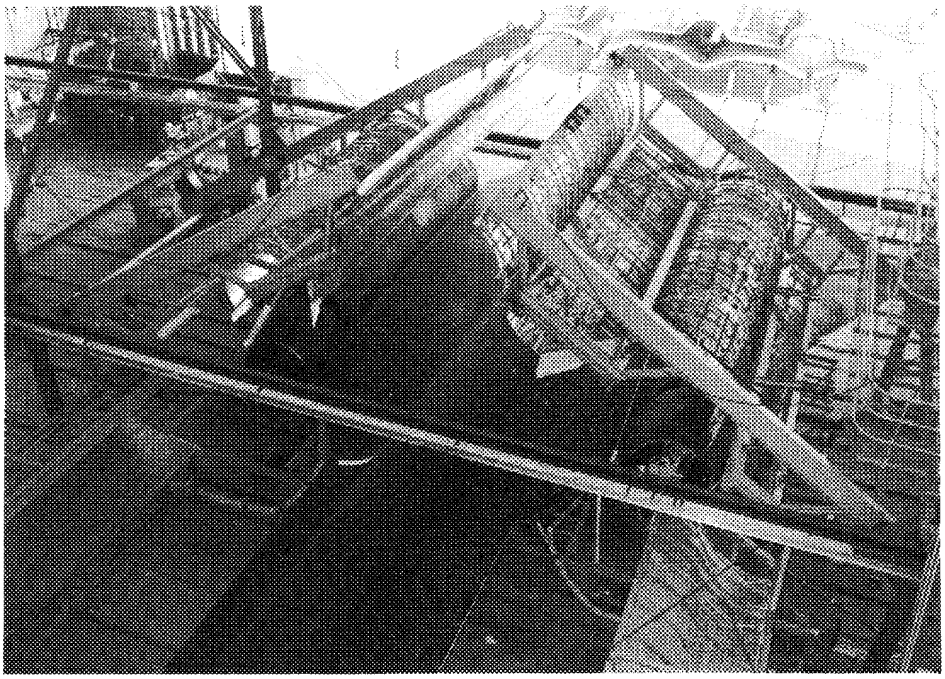

E-25406

Fig. 32: Retracted heater system

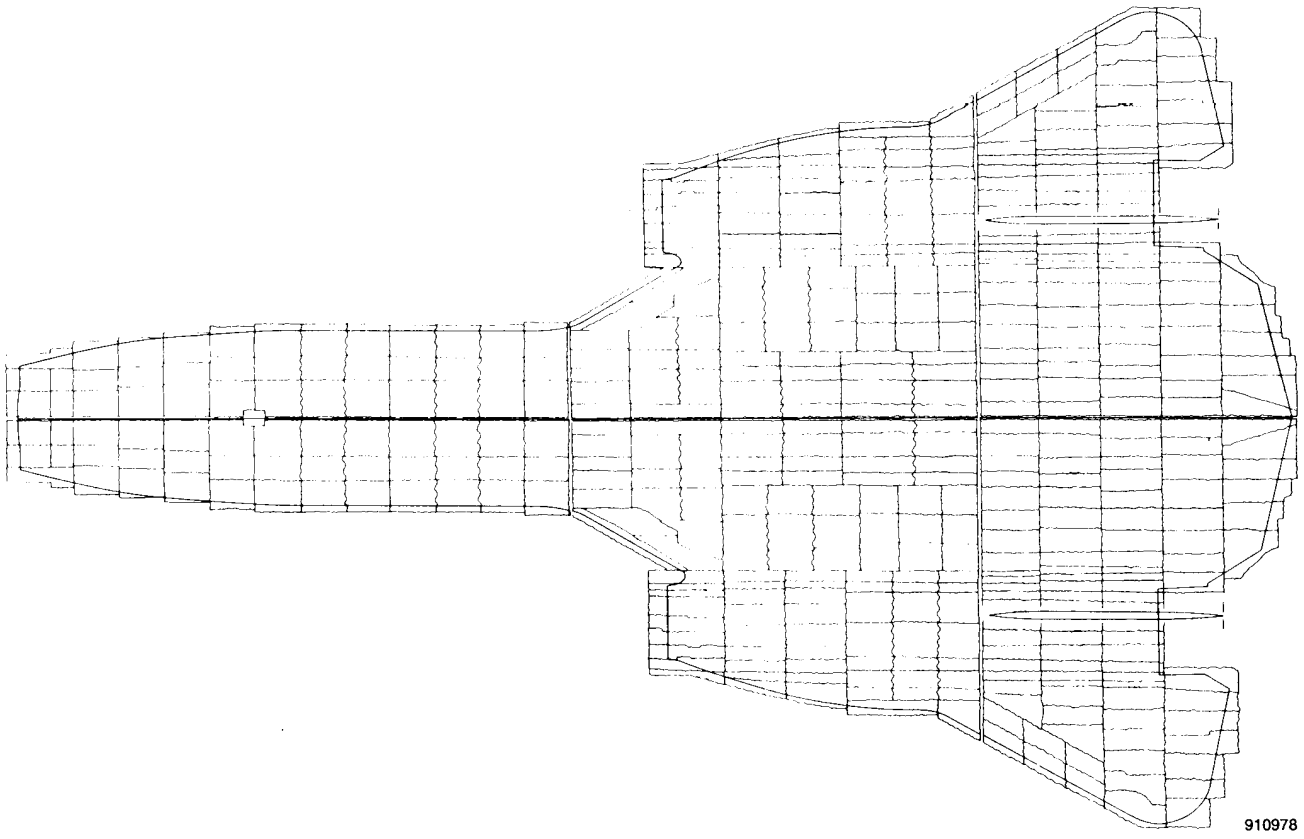

Fig. 33: Upper surface heater zoning

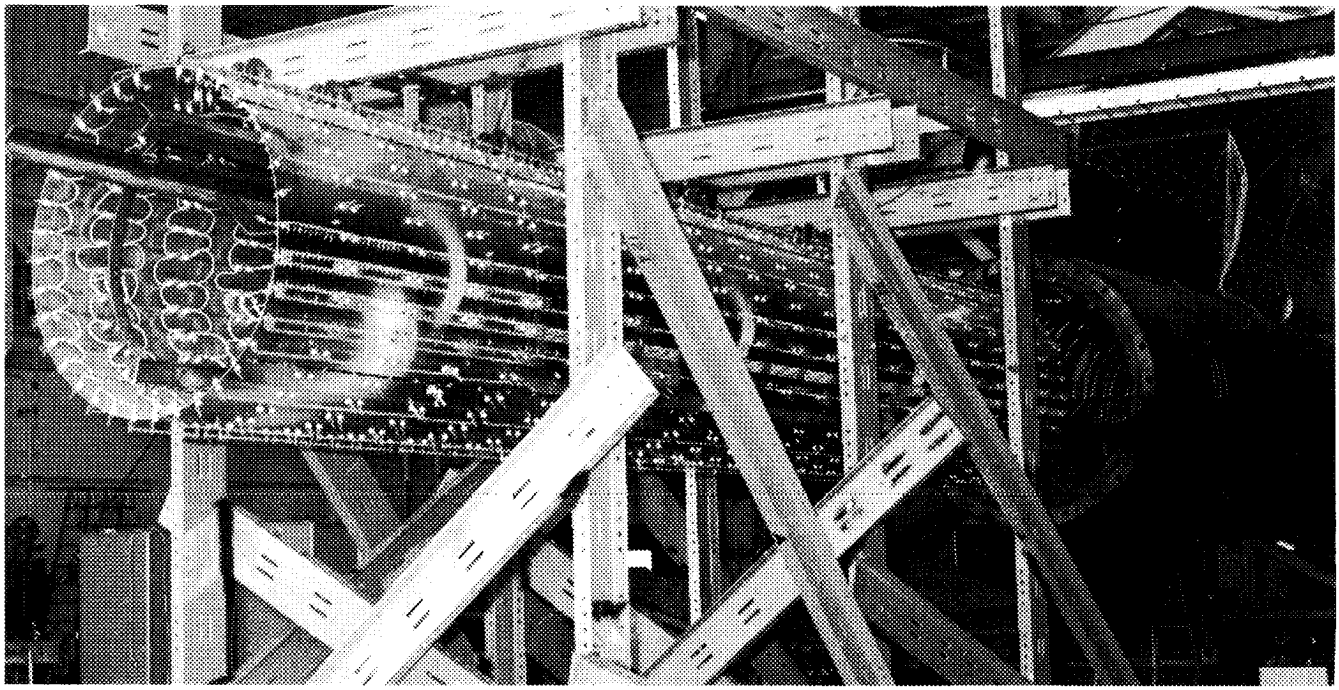

E-25459

Fig. 34: Internal nacelle heater

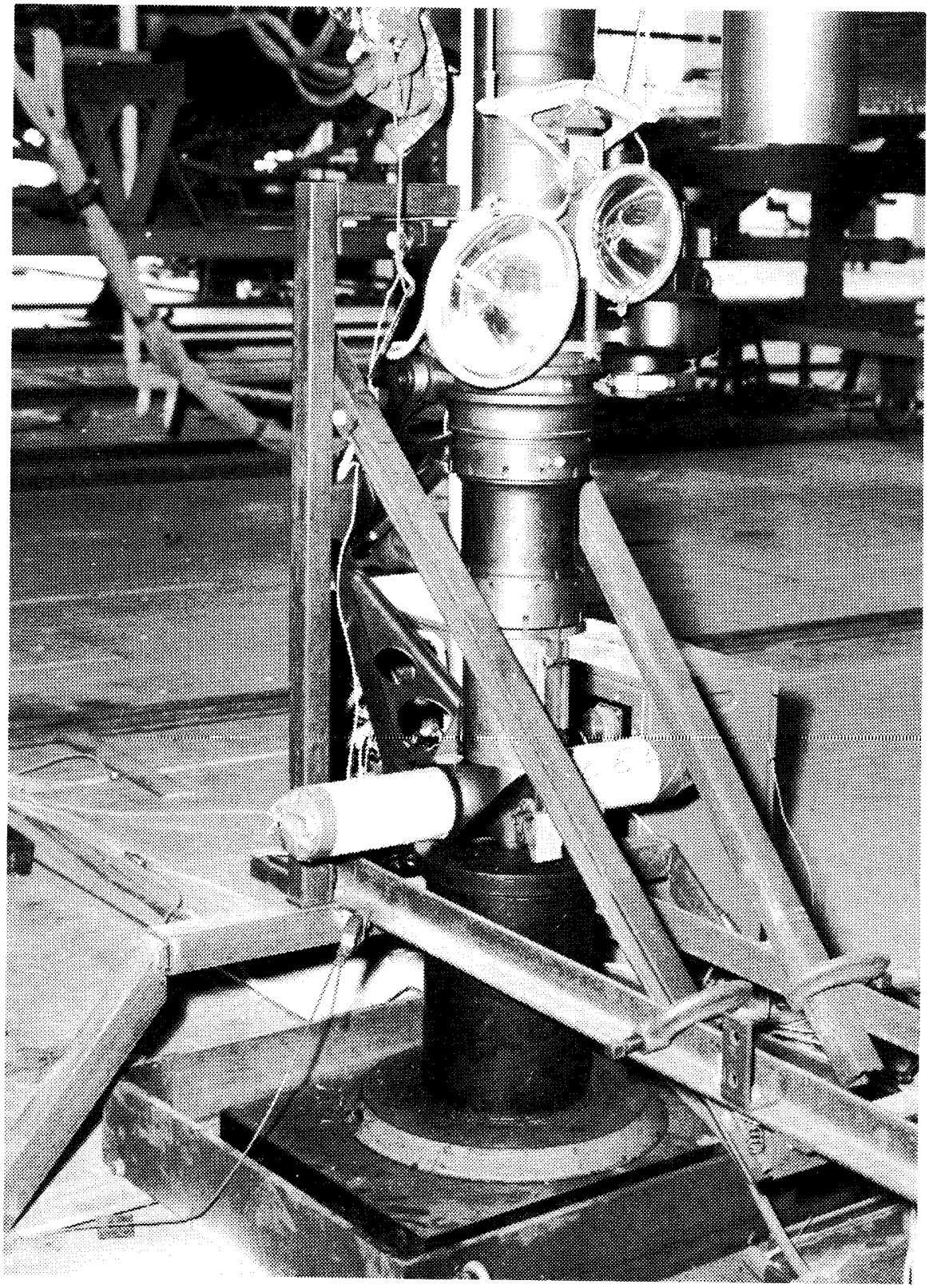

E-25425

Fig. 35: Nose gear support

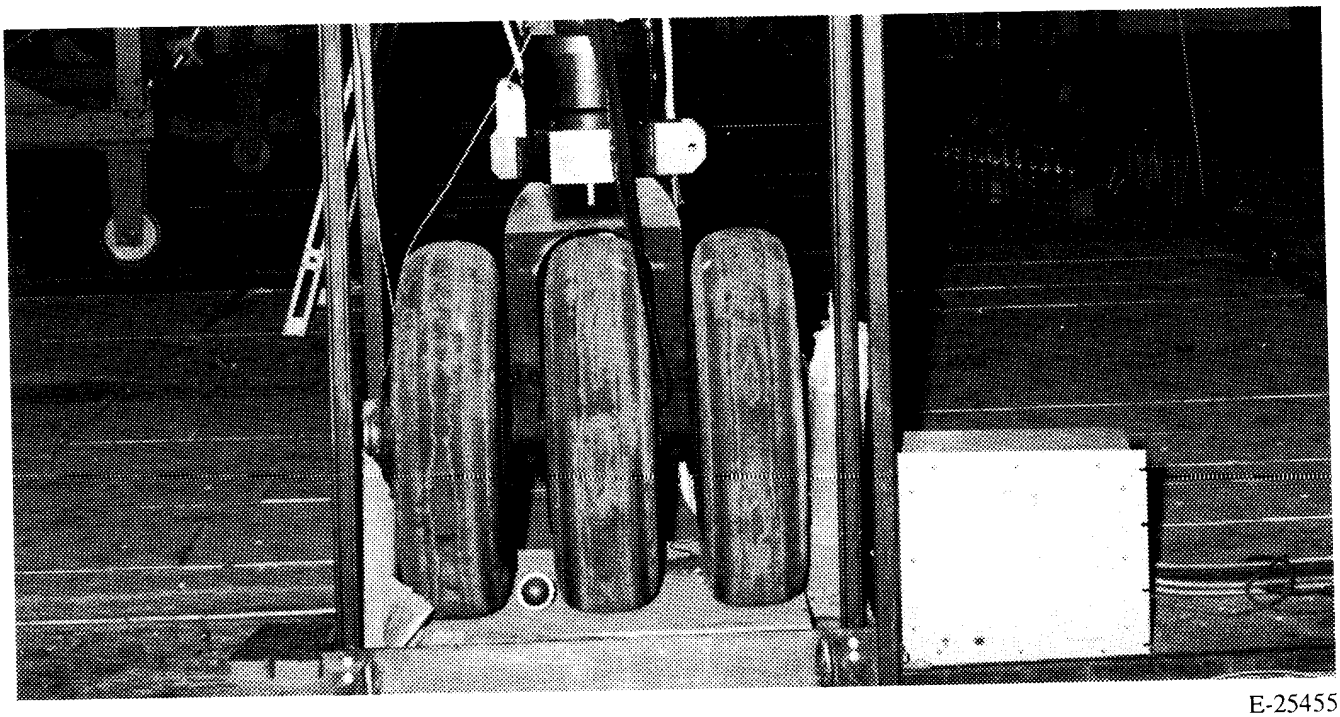

E-25455

Fig. 36: Left main landing gear support

REPORT DOCUMENTATION PAGE

Form Approved
OMB No. 0704-0188

1. AGENCY USE ONLY *(Leave blank)*	2. REPORT DATE	3. REPORT TYPE AND DATES COVERED
	January 1992	Technical Memorandum

4. TITLE AND SUBTITLE

Flight Vehicle Thermal Testing With Infrared Lamps

5. FUNDING NUMBERS

RTOP 505-63-50

6. AUTHOR(S)

Roger A. Fields

7. PERFORMING ORGANIZATION NAME(S) AND ADDRESS(ES)

NASA Dryden Flight Research Facility
P.O. Box 273
Edwards, California 93523-0273

8. PERFORMING ORGANIZATION REPORT NUMBER

H-1779

9. SPONSORING/MONITORING AGENCY NAME(S) AND ADDRESS(ES)

National Aeronautics and Space Administration
Washington, DC 20546-0001

10. SPONSORING/MONITORING AGENCY REPORT NUMBER

NASA TM-4336

11. SUPPLEMENTARY NOTES

Presented at the Structural Testing Technology at High Temperature Conference, November 4–6, 1991, Dayton, Ohio, Society for Experimental Mechanics, Inc., (SEM).

12a. DISTRIBUTION/AVAILABILITY STATEMENT

Unclassified — Unlimited
Subject Category 05

12b. DISTRIBUTION CODE

13. ABSTRACT ***(Maximum 200 words)***

The verification and certification of new structural--material concepts for advanced high-speed flight vehicles relies greatly on thermal testing with infrared quartz lamps. The basic quartz heater system characteristics and design considerations are presented. Specific applications are illustrated with tests that were conducted for the X-15, the Space Shuttle, and YF-12 flight programs.

14. SUBJECT TERMS

Infrared heating; Quartz lamps; thermostructural testing; high-temperature testing

15. NUMBER OF PAGES

32

16. PRICE CODE

A03

17. SECURITY CLASSIFICATION OF REPORT	18. SECURITY CLASSIFICATION OF THIS PAGE	19. SECURITY CLASSIFICATION OF ABSTRACT	20. LIMITATION OF ABSTRACT
Unclassified	Unclassified	Unclassified	Unlimited